

Fall 2006

Effects of STZ induced hyperglycemia and hyperlipemia on PPARgamma and ABCA1 in a hamster model of atherogenesis

Craig LaMarca

University of New Hampshire, Durham

Follow this and additional works at: <https://scholars.unh.edu/thesis>

Recommended Citation

LaMarca, Craig, "Effects of STZ induced hyperglycemia and hyperlipemia on PPARgamma and ABCA1 in a hamster model of atherogenesis" (2006). *Master's Theses and Capstones*. 203.

<https://scholars.unh.edu/thesis/203>

This Thesis is brought to you for free and open access by the Student Scholarship at University of New Hampshire Scholars' Repository. It has been accepted for inclusion in Master's Theses and Capstones by an authorized administrator of University of New Hampshire Scholars' Repository. For more information, please contact nicole.hentz@unh.edu.

**EFFECTS OF STZ INDUCED HYPERGLYCEMIA AND
HYPERLIPEMIA ON PPAR γ
AND ABCA1 IN A HAMSTER MODEL OF ATHEROGENESIS**

By

Craig LaMarca

Bachelor of Science, University of New Hampshire, 2004

THESIS

**Submitted to the University of New Hampshire
in Partial Fulfillment of
the Requirements for the Degree of**

**Master of
Science**

Animal Science

September, 2006

UMI Number: 1437632

INFORMATION TO USERS

The quality of this reproduction is dependent upon the quality of the copy submitted. Broken or indistinct print, colored or poor quality illustrations and photographs, print bleed-through, substandard margins, and improper alignment can adversely affect reproduction.

In the unlikely event that the author did not send a complete manuscript and there are missing pages, these will be noted. Also, if unauthorized copyright material had to be removed, a note will indicate the deletion.

UMI[®]

UMI Microform 1437632

Copyright 2006 by ProQuest Information and Learning Company.

All rights reserved. This microform edition is protected against unauthorized copying under Title 17, United States Code.

ProQuest Information and Learning Company
300 North Zeeb Road
P.O. Box 1346
Ann Arbor, MI 48106-1346

This thesis has been examined and approved.

Thesis Director, Thomas L. Foxall, Ph.D.
Professor of Animal and Nutritional Sciences
University of New Hampshire

Wendell P. Davis, DVM., Dipl. A.C.V.P.
Clinical Associate Professor
University of New Hampshire

Arthur F. Stucchi, Ph.D.
Research Associate Professor
Boston University Medical Center

August 14, 2006

Date

ACKNOWLEDGEMENTS

After six years of an intense , but gratifying academic experience in the Animal sciences department here at UNH, there are many people who have I interacted with that have aided in my experience and deserve my sincere gratitude.

Firstly, I have to thank Dr. Foxall, who has made this experience not only possible, but worthwhile, beneficial and enjoyable. Dr. Foxall's easy going attitude and sense of humor have made what should have been a stressful, intense two years into an amazing academic experience; not only as a mentor and advisor, but as a friend. His passion and drive for academic research have provided many, including myself, the ability to thrive in the field. Without him, I would certainly not be where I am at today, and probably would still be wondering what to do with my life.

Secondly, I would like to extend my gratitude to Adele Marone, whose extensive technical knowledge in the field proved very valuable to my success. Without her patience and time that she so kindly offered to me everyday while she taught me the technical skills I needed in the lab, my graduate career would have ceased to continue.

I would also like to sincerely thank my thesis committee members, Dr. Wendell Davis and Dr. Arthur Stucchi for their time, interest and support over the past two

years. On top of their already busy lives, they were willing to apply the time, effort and knowledge to guide me through my graduate career.

Last, but certainly not least, I would like to thank everyone in Kendall Hall, including all the great friends I have made during my time at UNH. I would especially like to thank the New Hampshire Veterinary Diagnostic lab for their assistance in processing my paraffin embedded tissue. Also, the administrative and library staffs have proven to be invaluable resources along the way.

Finally, I would like to thank my parents, Pat and Fred LaMarca who have been very supportive of me, not only during the last two years, but throughout the duration of my academic career. Their love and support has always been the backbone of my success.

TABLE OF CONTENTS

ACKNOWLEDGMENTS.....	iii
LIST OF TABLES.....	vi
LIST OF FIGURES.....	vi
ABSTRACT.....	viii
CHAPTER	PAGE
1. INTRODUCTION.....	1
2. EXPERIMENTAL DESIGN.....	34
3. MATERIALS AND METHODS.....	36
4. RESULTS.....	52
5. DISCUSSION.....	77
6. REFERENCES.....	88
7. APPENDIX A.....	99

LIST OF TABLES

1. <i>PPARγ and atherosclerosis</i>	26
2. <i>Hamster Weights</i>	59
3. <i>Plasma Glucose and Hemoglobin A1C</i>	60
4. <i>Plasma Total Cholesterol and Triglycerides</i>	60
5. <i>HDL/non-HDL Cholesterol and Total Cholesterol/HDL Ratio</i>	60
6. <i>Active PPARγ Expression (ELISA Results)</i>	61

LIST OF FIGURES

1. <i>Reverse Cholesterol Transport</i>	15
2. <i>PPAR Isoforms</i>	21
3. <i>ABCA1 in Reverse Cholesterol Transport</i>	27
4. <i>Experimental Design</i>	35
5. <i>Segments of the Hamster Aortic Arch</i>	41
6. <i>Hamster Weights</i>	62
7. <i>Hemoglobin A1C Values</i>	63
8. <i>Blood Glucose Concentrations</i>	64
9. <i>Plasma Total Cholesterol Values</i>	65
10. <i>Plasma Triglyceride Levels</i>	66
11. <i>Plasma HDL and non-HDL Cholesterol Concentration</i>	67
12. <i>TC/HDL Ratio</i>	68
13. <i>Histology-Hematoxylin and Eosin (Morphology)</i>	70
14. <i>Immunohistochemistry - Negative Controls</i>	72
15. <i>Immunohistochemistry - PPARγ</i>	74
16. <i>Immunohistochemistry - ABCA1</i>	76

ABSTRACT

EFFECTS OF STZ INDUCED HYPERGLYCEMIA AND HYPERLIPEMIA ON PPAR γ AND ABCA1 IN A HAMSTER MODEL OF ATHEROGENESIS

By

Craig J. LaMarca
University of New Hampshire, September 2006

Diabetes mellitus accelerates atherogenesis, but the exact mechanisms involved are unknown. This study examined the effects of hyperglycemia on the inflammatory transcription factor peroxisome proliferator activated receptor gamma (PPAR γ), known to be involved in atherogenesis, and the ATP binding cassette A1 (ABCA1) protein that is a downstream product of PPAR γ . ABCA1 is a membrane bound transporter that is involved in reverse cholesterol transport via high density lipoprotein cholesterol (HDL-C). Hamsters were divided into two groups; hyperlipemic animals fed a high fat/high cholesterol control diet (C) and hyperlipemic/hyperglycemic animals that received the high fat diet and were administered streptozotocin. Half of the hamsters (23) in each group were sacrificed at 8 weeks and the other half at 24 weeks. To determine the role of PPAR γ and ABCA1 in atherogenesis, aortas were harvested for ELISA, western blot and immunohistochemical analyses of PPAR γ and ABCA1. The 8 week hyperlipemic hamsters had lower total cholesterol levels than the 8 week treated hamsters and both groups at 24 weeks. At 8 and 24 weeks, the TG levels of the treated hamsters' were

elevated over controls, 24 week control values were higher than 8 week controls, but 24 week treated values were lower than at 8 weeks ($p < .05$). Hemoglobin A1C (HbA1C) levels were higher ($p < .001$) in both treatment groups as compared to the controls but there were no differences between time points. HDL-C levels were lower in the 24 week treatment hamsters compared to all other groups. Non-HDL cholesterol values were higher ($p < .05$) in treatment groups at both time points and 24 week controls were higher than 8 week controls. TC/HDL ratios were higher ($p < .05$) in both treatment groups as compared to controls and were higher ($p < .05$) in both groups at 24 weeks as compared to 8 weeks. Advanced fatty streak lesions were observed in the 8 week treatment group and in both the control and treatment hamsters at 24 weeks. The most advanced lesions were observed in the 24 week treatment animals. Both 8 week control and treated aortas as well as 24 week controls had mild focal reactions for PPAR γ and ABCA1 based on IHC, and while the 24 week treatment sections had multi-focal, intense immunoreactivity. Thus, based on the immunohistochemical and ELIAS analyses, the 24 week treated animals showed a greater expression of PPAR γ and ABCA1. Although activated PPAR γ was detected by ELISA in all groups, there were no statistical differences between groups. However, average 8 week treated values were higher than 8 week controls and 24 week controls were higher than both 8 week control and treated aortas. Treated values at 24 weeks declined as compared to controls. Due to extremely low protein concentrations, comparisons could not be made on western blot data although PPAR γ was detectable. Hyperglycemia as compared to hyperlipemia produced a more atherogenic lipid profile, more advanced arterial lesions, and observed increases in

PPAR γ and ABCA1 expression. The added metabolic stress of hyperglycemia in addition to hyperlipemia appeared to induce the further expression of PPAR γ and ABCA1, although the potential beneficial effects of this were outweighed by the extremely adverse lipid profile.

CHAPTER 1

INTRODUCTION

According to the American Heart Association, cardiovascular disease (CVD) is the leading cause of morbidity and mortality in the Western World [1]. In the United States alone, over 71 million American adults are living with one or more types of CVD and over 13 million of them have coronary heart disease (CHD) i.e., a coronary artery narrowing leading to hypoxia, inadequate nutrient provision and decreased metabolite removal [1]. CHD is also the leading cause of death in patients with type 2 diabetes, and the relative risk for developing CHD in diabetic patients is increased 2-4 fold [2]. Preliminary mortality data show that CVD was the underlying cause of over 37% of all deaths (2,444,000) in the United States in 2003, and over 58% of all deaths in 2002 [1]. The threat that CVD poses is certainly not a new one; CVD has been the number one killer in the US every year since 1900 with the exception of 1918, claims the lives of 2500 Americans each day, and is responsible for one death every 35 seconds [1].

It is now well known that atherosclerotic coronary artery disease is a major complication of diabetes mellitus, a disease that affects the lives of more than 14 million Americans [3]. One might assume that confounding variables might play a role in the increased incidence of CVD in diabetic patients, as a number of pre-defined risk factors for CVD such as elevated blood pressure and abnormal lipid profiles are more common in diabetics as compared to the general population. However, no more than 25% of the excess atherosclerotic risk from diabetes can be attributed to these known risk factors [4]. But, there is statistical evidence that CVD accounts for up to 80% of the deaths in

patients with type 2 diabetes mellitus. The connection has focused worldwide research on the connection between type 2 diabetes and the increased incidence of CVD in these individuals. Many mechanisms have been proposed as commonalities between these disease states, but none as prevalent or convincing as inflammation. Overall, hyperglycemia, the root cause of both type 1 and 2 diabetes mellitus, seems to exacerbate the mechanisms that contribute to the development of CVD. More specifically, platelet hyperaggregability and or increased platelet adhesiveness and coagulation abnormalities, in addition to hypertension, all contribute to the accelerated development of atherosclerosis seen in type 2 diabetics [5]. On the cellular level, the hyperglycemia, hyperinsulinemia, and proatherogenic dyslipidemia associated with diabetes all contribute to complex vascular interactions that induce the atherogenic process. The dyslipidemia often observed in diabetics is associated with elevated levels of small, dense low density lipoprotein (LDL-C) particles, low levels of high density lipoprotein (HDL-C) as well as elevated triglycerides (150 mg/dL or higher). Elevated levels of triglycerides (hypertriglyceridemia), which is associated with increased circulating levels of triglyceride-rich lipoproteins, has been implicated as a risk factor for atherosclerosis and progression of coronary artery disease [6]. Hypertriglyceridemia is one of the metabolic abnormalities commonly observed in insulin resistant individuals. Diabetics experience extensive metabolic abnormalities such as increased circulating levels of inflammatory markers including C-reactive protein (CRP), TNF- α , as well as increased expression of the pro-inflammatory adhesion molecules intercellular adhesion molecule (ICAM) and vascular cell adhesion molecule (VCAM). The extent of biochemical changes in diabetics is complex and not-yet fully understood. One widely studied aspect

of the biochemical abnormalities associated with insulin resistance and diabetes is the irreversible formation of advanced glycation end products (AGEs) with arterial wall proteins, lipids and nucleic acids. Increased circulating levels of AGEs and subsequent activation of their receptors (RAGE) on endothelial cells increases oxidative stress and activates protein kinase C, which eventually alters normal cellular function. The activation of the AGE-RAGE cascade induces the expression of adhesive molecules such as VCAM resulting in localization of circulating inflammatory cells to disease prone segments of the vasculature. This type of low-grade inflammation is a hallmark of diabetes which includes increasing circulating levels of inflammatory markers including CRP, fibrinogen, pro-inflammatory cytokines (TNF- α), adhesion molecules (ICAM and VCAM), IL-6 and a host of other inflammatory markers [7]. Hence, the association of inflammation with both the development of type 2 diabetes and atherosclerosis suggests a possible connection where by diabetes mellitus may accelerate the progression of atherosclerosis. This study will examine the effects of hyperglycemia on mediators of inflammation and dyslipidemia elucidating possible connections between the two disease states.

Diabetes Mellitus

About 21 million people, or 7 percent of the United States population, are currently living with some form of diabetes mellitus, and another 6 million people are estimated to be living unknowingly with the disease [8]. Type I diabetes mellitus, also referred to as insulin dependent diabetes, affects approximately 10% of all diagnosed cases, and is characterized by immunologic destruction of the insulin producing β -cells in

the pancreas [9]. Type I diabetes most often occurs early in life (aka: juvenile diabetes) and is characterized by two distinct, general pathologies; an immune mediated and an idiopathic form. The immune diagnosis is a result of an autoimmune attack on the pancreatic beta cells rendering them unable to carry out their normal physiological function of insulin production. The second pathology, idiopathic, implies that the reason for beta cell destruction is unknown, and is not associated with the production of antibodies [9].

Type II diabetes accounts for the other 90% of the diagnosed cases and is a dynamic disease characterized by a resistance to the effects of insulin leading to a hyperglycemic state [9]. Unfortunately, according to national diabetes statistics, the average onset of type II diabetes precedes clinical diagnosis by several years [10]. To the patient, this means that the detrimental effects of the hyperglycemic state will take place prior to diagnosis and treatment. Over the past thirty years, a rising incidence in cases of type II diabetes can be attributed to an increase in prevalence of obesity and a general decline in physical activity [9]. Type 2 diabetes is characterized by an altered lipid profile and an overall pro-inflammatory state. Both excess fat and diminished physical activity are predisposing factors to type II diabetes, or more specifically insulin resistance. Insulin resistance (IR) is defined as the inability of peripheral tissue to take up endogenous glucose in response to normal, circulating levels of insulin. The primary cause of the common form of type 2 diabetes is not completely understood, but autoimmune mechanisms are not involved [11]. Cellular resistance to the effects of insulin is a factor in 60-80% of individuals with type 2 diabetes. Decreased beta cell responsiveness to plasma glucose levels is observed, along with abnormal glucagon secretion and beta cell

dysfunction and eventual beta cell “burnout”. The islet dysfunction may be caused by a decrease in beta cell mass, abnormal function of the beta cells, alterations in the insulin receptor, or post-receptor events. Pancreatic changes among type II diabetic patients tend to be non-specific and in about 30% of these patients the changes are associated with increased amyloid deposition which can also lead to islet cell destruction. On top of detrimental pancreatic changes, liver changes related to elevated serum lipid levels are also observed in type 2 diabetics. Pancreatic and hepatic atrophy, although observed in diabetics and non-diabetics, occurs amongst diabetics with much greater frequency, and this increase in fatty infiltrates may also play a role in the development of amyloid deposits in the islets. Eventual pancreatic fibrosis also plays a role in loss of beta cell function in about 50% of individuals with type 2 diabetes [11]. This decreased beta cell function leads to the advanced stages of type II diabetes characterized by decreased or diminished insulin secretion, insulin resistance (IR) and hyperglycemia.

Dyslipidemia and the Metabolic Syndrome

The observation that IR, as well as a number of other risk factors, such as obesity, hypertension and hypercholesterolemia are common in those who are predisposed to the development of cardiovascular disease lead to the suggestion of a metabolic syndrome, or a group of symptoms that collectively indicate an increased risk to CVD. Much debate and controversy has arisen over the idea of classifying a clustering of risk factors for cardiovascular disease. It is still vague how the syndrome should be represented and how the underlying mechanisms of the syndrome affect the predisposition to cardiovascular disease[12]. Generally, the metabolic syndrome clusters hypertension, dyslipidemia,

impaired glucose tolerance and obesity, which are all well established risk factors for CVD. This clustered phenotype has been discussed since the 1980s as the “metabolic syndrome”, but prior to that, as early as the 1930s, it was described as syndrome X, the insulin resistance syndrome, and the deadly quartet [13]. More recently, due to the concept of metabolic abnormality or dysfunction within the syndrome, some authors have suggested the use of the dysmetabolic syndrome. There have been numerous attempts to standardize the definition of the metabolic syndrome, but no final definition has been established. One of the most widely used definitions, developed by the World Health Organization (WHO) in 1998 and revised in 1999, establishes that the human metabolic syndrome requires at least one of the following: type II diabetes mellitus or impaired glucose tolerance or glucose resistance. It also requires at least two of the following: hypertension (BP > 140/90 mm Hg), obesity (body mass index [BMI] \geq 30 kg/m², or waist to hip ratio > 0.90 for male subjects or > 0.85 for female subjects), dyslipidemia (low HDL-C cholesterol [$<$.90mmol/L] and/or hypertriglyceridemia (\geq 1.7 mmol/L), or microalbuminuria (urinary albumin excretion rate > 20ug/min) [14]. The estimates of current prevalence among various populations are alarming and projections are for future increases. According to the National Health And Nutrition Examination Survey III (NHANES III), from 1988 to 1994, 24% of adult Americans older than 20 years had the syndrome [15]. A recent study by Isomaa et al. reported that there is a 3-fold excess of CHD and stroke in subjects with the metabolic syndrome phenotype [16]. It has been estimated that 75% of people with type II diabetes meet the criteria for the metabolic syndrome, and many believe that obesity is a key etiologic factor in the development of the underlying insulin resistance [17]. Much effort and time has been spent toward the

therapeutic treatment of the individual components of the metabolic syndrome, and many successful treatments have been developed. Physicians and pharmaceutical companies have targeted high blood pressure for the treatment of CVD for many years and have been relatively successful at producing drugs efficient at lowering hypertension. With the introduction of statins and advice on total lifestyle changes (TLC), the medical world has been able to target and decrease elevated LDL-C levels, but unfortunately these changes have not lead to concomitant decreases in incidence of CVD. The reasons for this discord are primarily unknown and have caused researchers to focus their studies on other risk factors. More recently, effort has been put toward treating the other abnormalities associated with dyslipidemia and insulin resistance; more specifically, a lower concentration of serum HDL-C cholesterol that is observed in this state.

The HDL-C Hypothesis

Epidemiological studies have identified elevated LDL-C as an independent risk factor for cardiovascular disease. Over the past ten years, clinical trials aimed at lowering LDL-C to decrease CVD risk have plainly established that reductions in LDL-C are associated with 30% to 40% reductions in clinical events [18]. Unfortunately, despite the efficacy of statins and other drugs in lowering serum LDL-C levels, many patients continue to experience detrimental cardiovascular events. Because the efficacy of targeting LDL-C to decrease CVD risk is still questionable, research has also been directed toward pharmacological, genetic, and dietary manipulations to raise serum HDL-C. Non-epidemiological studies have shown evidence that raising HDL-C could reduce the risk of CVD. One study, using transgenic animals that overexpress apolipoprotein A1

(apoA1), showed that increasing plasma HDL-C protected against diet induced and genetically determined atherosclerosis [19]. In another study, infusion of HDL-C in the form of apoA-1/phospholipids complexes was associated with regression of atherosclerosis in cholesterol fed rabbits [20]. This is important because by increasing HDL-C, not only can physicians target the initiation and progression of the disease, but they might actually be able to regress the progression of atherosclerotic lesions. In another study, 5 weekly infusions of apoA-1 Milano/phospholipid complexes in healthy men were shown to decrease total atheroma volume by 4.2% after an acute coronary event using intravascular ultrasound to quantitate coronary atheroma. These results all point at the fact that raising plasma levels of HDL-C could significantly decrease the onset and outcome of severe cardiovascular events. More clinical trials need to be carried out to measure surrogate endpoints of atherosclerosis, especially considering some of the disappointing results of the LDL-C trials after some promising initial results. If some of the rate limiting enzymes or integral proteins involved in HDL-C synthesis and processing could be up-regulated, hypothetically some of the associated risks of low serum HDL-C could be diminished.

The next step towards development of therapeutic options based on increasing HDL-C levels is understating the atheroprotective nature of the HDL-C molecule itself. Although our knowledge of its actions are not complete, there is evidence to support at least three atheroprotective mechanisms. HDL-C mediates the efflux of cholesterol from peripheral cells (eg: arterial macrophages) in order for cholesterol to be returned to the liver for processing (breakdown and bile acid conversion). Cholesterol efflux from macrophages within the atheroma to the HDL-C molecule can occur by passive diffusion

[21], by combining with the scavenger receptor B1 (SR-B1) [22] or by binding to the ATP Binding Cassette Transporter A1 (ABCA1) [23-25]. Nascent apoA is the preferred acceptor for the ABCA1 transporter mediated cholesterol efflux which after esterification of free cholesterol to cholesteryl esters (CE) by lecithin cholesterol acyltransferase (LCAT) is then converted to spherical α -HDL-C [26] (see figure 1). HDL-C is a pivotal component of the atheroprotective reverse cholesterol transport pathway, functioning as the shuttle of excess peripheral cholesterol to the liver for disposal as bile acids and cholesterol. A second major mechanism by which HDL-C may be protective against the progression of atherosclerosis is by protection of LDL-C from oxidation. Oxidatively modified LDL-C, unlike normal LDL-C, is recognized by scavenger receptors CD36 and SRA on macrophages resulting in the macrophage accumulation of CE and incidental foam cell formation. Oxidized lipids are transferred from LDL-C to HDL-C and are hydrolyzed by HDL-C paraoxonase and PAF acetylhydrolase [27]. A third mechanism by which HDL-C may protect against the onset of CVD is the selective decrease of endothelial cell adhesion molecules, which facilitate the binding of monocytes to the vessel wall subsequently promoting lesion development [28]. In order to elucidate the specifics of these mechanisms, it is important to know some of the basics of atherogenesis, and the role of reverse cholesterol transport.

Pathogenesis of Atherosclerosis

The normal arterial wall consists of three well-defined concentric layers; the innermost layer is the tunica intima, the middle layer is the tunica media, and the outermost layer is known as the tunica adventitia. These three layers are separated by

concentric layers of elastin known as the external and internal elastic lamina. [3] The luminal surface of arteries is lined by a single contiguous layer of endothelial cells that rests upon a basement membrane superficial to the tunica intima. At one time, atherosclerosis was thought of as a passive process of lipid accumulation and plaque formation causing the endothelial cells to reflexively protrude into the luminal space. It is now known that atherosclerosis is a multi-factorial, dynamic process in which the endothelial cells regulate a wide variety of functions in the arterial wall including thrombosis, vascular tone, and leukocyte trafficking. Throughout the years, atherosclerosis has been characterized in many ways including: a degenerative disease process, a proliferative process and an accumulative process. One of the most widely accepted views is the “response to injury” hypothesis which was modified and tested by Russel Ross. This hypothesis implies that the lesions represent a specialized form of a “protective, inflammatory-fibroproliferative response to various forms of insult to the arterial wall.” Depending on the extent and duration of the insult, the defensive response may become chronic and excessive leading to a disease process [29].

In human atherosclerosis is characterized by three lesion stages: fatty streak, fibro-fatty and advanced. Fatty-streak lesions are characterized by nodular areas of lipid deposition; these early lesions, characterized by the development of macrophage ‘foam cells’ typically start by the age of 10, and increase to involve as much a 1/3 of the aortic surface in the third decade of life [3]. The production of these lipid-loaded macrophages which contain large amounts of CE is a hallmark of both early and late atherosclerotic lesions. The accumulation of cholesterol in these cells is thought to be mediated primarily by the uptake of modified forms of LDL-C via scavenger receptors (e.g., CD36 and SRA)

[30]. Although there may be multiple proteins that aid in the cholesterol uptake, scavenger receptors A (SRA) and CD36 have been shown to play significant, quantitative roles. Research with Apo E-deficient mice lacking the SRA and CD36 receptors has demonstrated that these animals develop significantly less atherosclerosis than control Apo E knockout mice [31]. Cholesterol taken up by the macrophage via scavenger receptors in the oxLDL-C form consists of free cholesterol as well as lysosome hydrolyzed cholesterol esters. Free cholesterol has a number of metabolic fates, including esterification by acyl coA:cholesterol acyltransferase (ACAT) as well as storage within the lipid droplets that characterize foam cells. Cholesterol deposits within these lipid droplets can in turn be hydrolyzed by cholesterol ester hydrolase, generating free cholesterol for incorporation into membranes as well as for transport out of the cell. The fate of cholesterol, once hydrolyzed, will be discussed in detail later, but involves two main processes: enzymatic modification to more soluble forms and efflux via membrane transporters.

As fatty streak lesions progress, there is a transition from the relatively simple fatty-streak to a more complex lesion, which is characterized by the transmigration of smooth muscle cells (SMCs) from the medial layer through the internal elastic lamina and into the intimal, or subendothelial space. These smooth muscle cells, now located in the intimal space have the ability to proliferate and take up modified lipoproteins, further contributing to foam cell formation. These SMCs also begin to produce and secrete extracellular matrix proteins that strengthen and enlarge the plaque and form the beginnings of the fibrous cap [32, 33]. The lesion has now entered a phase of development that is influenced by interactions between monocytes/macrophages and T cells that result in a

wide range of humoral and cellular responses. The lesion is in a self-perpetuating chronic inflammatory state: lesional T cells appear to be activated expressing both Th1 and Th2 cytokines [34]. Pro-inflammatory cytokines produced within the atheroma provide a chemotactic stimulus to migrating leukocytes directing their adherence and migration into the intimal space. Once these blood-derived inflammatory cells are resident in the arterial wall, they sustain the local inflammatory response. As progression continues, T-cells are further stimulated, encountering protein antigens such as oxLDL-C, heat shock protein 60 (HSP60), microbial antigens and simultaneous ligation of costimulatory receptors. The antigenic stimulation causes them to elaborate the production of pro-inflammatory cytokines such as γ -interferon and TNF α . These cytokines can in turn stimulate macrophages proliferatively and phenotypically as well as vascular endothelial cells and SMCs. As this inflammatory process is perpetuated, the activated leukocytes and endogenous arterial cells can release fibrogenic mediators including a variety of growth factors that can promote proliferation of SMCs. As the SMCs proliferate and concentration of fibrogenic mediators increases, so does the extent of elaboration of the extracellular matrices becoming more characteristic of the advanced lesion.

Advanced lesions are characterized by a necrotic core, with increased calcified fibrous areas of the artery with visible ulceration. Inflammatory processes not only promote induction and evolution of the atherosclerotic plaque, but also contribute definitively to the acute thrombotic complications of atheroma [35]. Although the advanced lesion can lead to ischemic disease as a result of progressive narrowing of the arterial lumen, acute cardiovascular events that result in myocardial infarction and stroke (the major sequella of lesion formation) are believed to result from plaque rupture that

leads to thrombosis[36]. If the plaque is unstable and ruptures, plaque material including lipids and tissue factor (TF) are exposed to blood, initiating the coagulation cascade, platelet adherence and thrombosis. The highly concentrated, activated macrophages within the arterial lesion can produce proteolytic enzymes (e.g., matrix metalloproteinases (MMPs)) that are capable of degrading the collagen and extracellular matrix that aids in strengthening the plaque's protective fibrous cap, rendering that cap thin, weak and susceptible to rupture. γ -interferon, also produced by activated macrophages, can stop production of collagen by SMCs, limiting their capacity to further produce strengthening extracellular matrix proteins. As the lesions further progress toward the most advanced state, apoptosis and necrosis of lipid-laden macrophages becomes morphologically evident. The cell death going on within the arterial lesion can result from cell to cell interactions and the highly concentrated cytokine environment; it can involve the actions of pro- and antiapoptotic proteins that include death receptors, proto-oncogenes, and tumor suppressor genes [37]. The release of insoluble and oxidized lipids from necrotic cells leads to the formation of the extracellular lipid "gruel" seen in advanced lesions.

Reverse Cholesterol Transport

Almost all animal cells synthesize cholesterol and import cholesterol from plasma lipoproteins in order to maintain normal function. At any time, there is a dynamic between the amount of free cholesterol and CEs within the cell, which is regulated by lipid metabolic enzymes: acyl-coenzyme A: cholesterol acyltransferase-1 (ACAT1) and neutral cholesterol ester hydrolases (nCEH) also known as hormone sensitive lipase

(HSL). To maintain cholesterol balance and prevent cholesterol overload, cells must have the ability to export excess cholesterol. The only available reservoir for exported cholesterol deposition is the liver, owing its unique ability to synthesize bile acids and to transport cholesterol into bile. The process by which extrahepatic tissue controls the balance of cholesterol through its return to the liver is termed “reverse cholesterol transport (RCT).” In order to further study some of the key mediators involved in this protective mechanism in more detail, it is important to be able to understand the sequence of events in the reverse cholesterol transport process. Extrahepatic tissues, such as arterial tissue, synthesize cholesterol and also derive cholesterol through the uptake of lipoproteins via the LDL-C receptor and scavenger receptors. The cholesteryl esters in peripheral tissue are in a constant equilibrium with free cholesterol, through the opposing actions of ACAT and neutral cholesterol esterase. Free cholesterol (FC) is extruded to extracellular acceptors, most notably phospholipid/apoA-I disks (pre- β -HDL-C). This process is directly dependent on functional ABCA1, a membrane bound cholesterol shuttle. Proper cholesterol loading is essential for the stability of HDL-C, the primary lipoprotein involved in reverse cholesterol transport. In the absence of sufficient cholesterol efflux, apoA-I is rapidly cleared from the circulation by the kidneys [38]. Cholesterol that associates with apoA-I/phospholipid disks is a substrate for LCAT, which transfers a fatty acyl chain from phosphatidylcholine to cholesterol, forming CE. The CE partitions into the hydrophobic core of the lipoprotein, thus forming spherical HDL-C particles. These particles can then deliver CE to the liver as well as to steroidogenic tissues. The interaction of spherical HDL-C particles with the scavenger receptor SR-BI leads to selective delivery of CEs, as the SRB1 receptor can only interact

with spherical HDL-C particles. The CEs are hydrolyzed by a neutral cholesterol esterase, providing free cholesterol for secretion across the apical (bile canalicular) membrane of the hepatocyte and for bile acid synthesis. (See Figure 1)

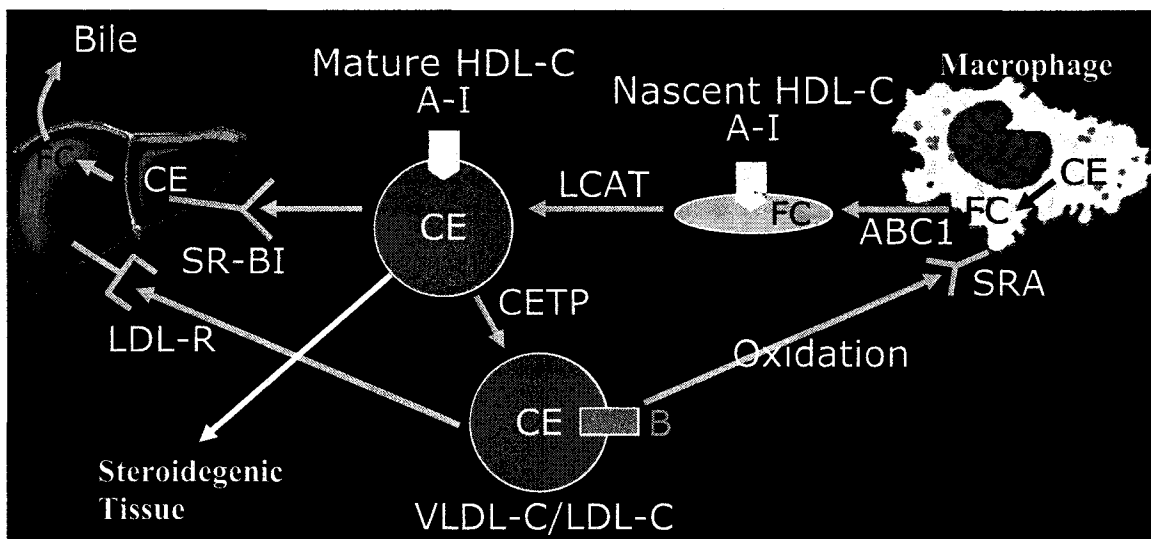


Figure 1: Reverse Cholesterol Transport

Derived from LipidsOnline.com

CE=Cholesteryl Ester, HDL-C=High Density Lipoprotein-Cholesterol, VLDL-Very Low Density Lipoprotein, LDL-C=Low Density Lipoprotein, LDL-R= Low Density Lipoprotein Receptor, FC=Free Cholesterol, SRBI=Scavenger Receptor B1, SRA=Scavenger Receptor A1, ABCA1=ATP Binding Cassette A1, LCAT=Lecithin cholesterol acyltransferase, CETP=Cholesteryl Ester Transfer Protein.

Transcription Factor Control

Transcription factors comprise a family of structurally-related eukaryotic proteins that are involved in the control of a large number of normal cellular and organismal processes, such as immune and inflammatory responses, developmental processes, cellular growth, and apoptosis. In addition, these transcription factors are persistently active in a number of disease states, including cancer, arthritis, chronic inflammation, asthma, neurodegenerative diseases, and heart disease. One factor, Nuclear Factor Kappa-

β (NF- κ B), has been implicated in the pathogenesis of both atherosclerosis and diabetes mellitus, primarily due to its control of inflammatory gene expression [39]. NF- κ B is a protein heterodimer, whose activation can be stimulated by a number of factors including: high glucose concentrations, free radical formation, TNF- α , radiation and other stimuli. Some of the many downstream consequences of NF- κ B activation include transcriptional synthesis of pro-inflammatory molecules and mediators of their expression including: increased expression of adhesion molecules like VCAM-1 and ICAM-1, tissue factor (TF) and the receptor for advanced glycation endproducts (RAGE). Activation of NF- κ B occurs in endothelial cells exposed to high glucose levels and low shear stress, but not in endothelial cells which are exposed to hyperglycemia without decreased shear flow [40]. Due to decreased shear flow at lesion prone areas, increased expression of NF- κ B at these sites might persist, leading to the increased synthesis of proteins involved in atherosclerotic progression and inflammation including VCAM-1. This inflammatory connection, could in part, explain the increased atherosclerosis in diabetic patients. Therapeutic control of NF- κ B might seem like a promising option due to its involvement both in inflammatory control and atherosclerotic progression; unfortunately specifically targeting vascular NF- κ B is not currently an option and complete inhibition of this gene would have detrimental systemic side effects [41].

The extensive knowledge of NF- κ B signaling also exposes the extent of research that still needs to be carried out in order to fully understand the pathway. Overexpression studies in-vitro almost certainly do not accurately reflect physiological signaling events, and more comprehensive studies looking at clinical endpoints need to be done. Studies in

Drosophila have shown that very small differences in nuclear concentrations of these factors, in their affinities for target DNA sites, and in cooperation or competition between other transcription factors can have profound physiological consequences [42]. In many situations, it is not known how or which of the many genes induced by NF- κ B in a given response contribute acutely to that response. The development of methods to analyze genome-scale changes in gene expression (e.g., cDNA microarrays), has already begun to uncover additional NF- κ B-responsive genes and has helped to clarify which NF- κ B target genes are activated in a given response. Earlier, unpublished work in our lab, by Gowdy et al. established that the combination of a hyperlipidemic and hyperglycemic condition in the Syrian golden hamster is associated with increased levels of mediators of inflammation, specifically RAGE, VCAM, and NF- κ B. This study sought to extend the work by Gowdy et al., by determining expression of other inflammatory transcription factors and their regulated proteins in the hyperglycemic Syrian hamster.

Peroxisome Proliferator Activated Receptors (PPARs)

Originally discovered as regulators of peroxisome proliferation in rodent livers in response to xenobiotics, peroxisome proliferator activated receptors (PPARs) are now known as members of the nuclear receptor super-family of ligand-activated transcription factors, which also include retinoic X receptor (RXR), and vitamin D receptor [43]. The PPARs are among a group of forty-eight nuclear receptors in the human and mouse genomes that have been discovered thus far [44]. The nuclear receptors are divided into three groups based on the identification of known ligands. In general, these receptors contain similar characteristics which include a ligand-independent transcriptional

activation function domain (AF-1) located on the N terminus, a core DNA-binding domain consisting of two highly conserved zinc finger motifs that are responsible for binding the receptor to specific DNA sequences, a hinge region that allows flexibility of the receptor to dimerize to other nuclear receptors and bind to DNA, a ligand binding domain (LBD) and a second dimerization interface, and lastly a second ligand dependent activation function domain (AF-2) at the carboxy terminus [45]. The three groups of nuclear receptors segregated based on known ligands, their target genes, and their physiologic function are: 1) the endocrine receptors, 2) the adopted orphan receptors, and 3) the orphan receptors. The PPARs are members of the “adopted orphan receptors,” that once activated through ligand binding, undergo a conformational change, heterodimerize with (RXR), and bind to PPAR response elements (PPRE) in the promoter region of target genes, thus modulating genetic expression in either a positive or negative fashion. The PPRE consists of a direct repeat of the consensus hexamer AGGCTA separated by one or two nucleotides [46, 47].

Three subtypes of PPAR exist (α , β/δ , and γ) encoded on separate genes and exhibiting different tissue-specific distributions (See figure 2). PPAR α is mainly expressed in heart, muscle, kidney and liver; it is responsible for the regulation and expression of genes involved in fatty acid oxidation. Fibrates are synthetic ligands of PPAR α used in the treatment of dyslipidemia, while polyunsaturated fatty acids and arachidonic acid metabolites, such as leukotriene B₄ are natural ligands of PPAR α . PPAR β/δ is the most ubiquitously expressed of the PPARs and also plays a role in lipid metabolism, specifically within cardiac tissue [48]. Of the three subtypes, little is known about PPAR β/δ and much debate surrounds the role this transcription factor in the

development and modulation of atherosclerosis with strong arguments on both the pro- and anti- atherogenic sides. One study reported that treatment of LDL-C $-/-$ mice with the potent PPAR β/δ agonist, GW0742X, reduces atherosclerosis lesion burden, as well as expression of pro-inflammatory proteins indicating the beneficial effects of agonizing the β/δ receptor in the treatment of atherosclerosis [49]. Further studies assessing the ability of PPAR β/δ agonists to diminish lesion stability and regress lesion size will provide more information in the efficacy of targeting this receptor in treatment of atherosclerosis.

PPAR γ encodes three major messenger RNAs (mRNAs) resulting from differential promoter usage and alternative splicing that results in two different protein isoforms differing in a 28 amino acid extension of unknown function at the amino terminus [50, 51]. PPAR γ 2 is mainly expressed in adipose tissue, whereas PPAR γ 1 is found ubiquitously, including in the liver, heart, kidney, endothelium, vascular smooth muscle cells, and macrophages, as well as other tissues. PPAR γ has been described as having important roles in lipid metabolism, cellular differentiation, atherogenesis, and glucose homeostasis[52]. PPAR γ 's involvement and importance in glucose homeostasis is demonstrated by the fact that the insulin sensitizing thiazolidinediones (TZDs) are synthetic high-affinity ligands of the PPAR γ receptor. TZDs are extremely important in the treatment of type 2 diabetes due to their ability to promote insulin sensitivity. The use of pioglitazone and rosiglitazone, two synthetic PPAR γ ligands, results in increased peripheral glucose use, reduced hepatic glucose output, and improvement in overall glycemic control. The activity of PPARs is primarily mediated by the binding of natural and synthetic ligands, although its activity is not limited to ligand activation. Transcriptional activity of the PPAR receptors can be influenced by other post-

translational modifications such as phosphorylation and ubiquitination [53]. PPARs also have the ability to transrepress multiple inflammatory pathways. This transrepression involves interaction with coactivators and corepressors including such factors as NF κ B, AP-1, signal transduction activated transcription factors, CCAAT/enhancer-binding protein and nuclear factor of activated T cells. Still today, much work needs to be carried out looking at the interactions of PPAR γ with other inflammatory transcription factors to elucidate the pathways involved as well as to uncover future therapeutic targets.

Besides their effects on carbohydrate metabolism and overall glycemic control, PPAR γ ligands have also been shown to have beneficial effects on plasma lipids, important molecules in the progression of atherosclerosis. PPAR γ is expressed in the endothelium [54], macrophages [23], and human atherosclerotic lesions [55] and has been shown to be expressed in almost every stage of atherosclerosis development and progression (See table 1). As well as being expressed ubiquitously throughout atherosclerotic tissue, PPAR γ agonists have also been shown to have pleiotropic vascular effects. When PPAR γ agonists are administered for the treatment of type 2 diabetes, the beneficial effects on cardiovascular disease risk may be attributed to the indirect effects on insulin resistance, a direct inhibitory effect on atherogenesis and endothelial cell dysfunction, as well as a potent antiinflammatory effect on molecules such as monocyte chemoattractant protein-1 (MCP-1) and C-reactive protein (CRP). So, the ability of PPAR γ and its agonists to regulate the atherosclerotic process might potentially be a complex, coordinated interaction between the indirect effects of PPAR γ activation on improving insulin sensitivity and reducing inflammation; this effect might also be coupled with PPAR γ 's ability to regulate glucose and fat metabolism.

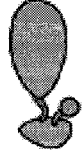


	PPAR α	PPAR γ	PPAR δ
			
Tissue Expression	Liver Heart Kidney Adrenal	Adipose tissue Spleen Adrenal Colon	Many tissues
Cell-specific Expression	Endothelial cells Macrophages Smooth muscle cells	Macrophages T cells Smooth muscle cells	Many cell types
Biological Functions	Triglyceride-rich lipoprotein synthesis and metabolism β -oxidation Anti-inflammation	Fat cell development Glucose homeostasis Anti-inflammation	Energy utilization Lipid metabolism Anti-inflammation
Endogenous Ligands	PUFAs 8(S)-HETE	PUFAs 15d-PGJ2 13-HETE 9-HODE	PUFAs Carboprostacyclin
Disease targets	Hypertriglyceridemia	Type 2 diabetes	Metabolic syndrome?
Drugs	Fibrates	Glitazones	

Figure 2: PPAR Isoforms

Adopted from Li et al.[45]

Initial work by Marx et al.[56] brought attention to PPAR γ and its role in atherogenesis. Further work by Marx observed increased expression of PPAR γ within both endothelial cells and vascular smooth muscle cells that were involved in atherosclerotic plaques of human coronary arteries [46, 57]. As stated, the initial concept was that this inflammatory transcription factor is being activated in all of the cell types

involved in the development and progression of atherosclerosis. The research began to shift towards the reasons why PPAR γ was being expressed in the human atheroma. The following year (1999), Yoshimoto et al. [58], using Wistar rats, clearly demonstrated that PPAR γ ligands are powerful inhibitors of vascular smooth muscle cell proliferation and that they may be a target for the treatment of neointimal hyperplasia. In early 2001, Collins and associates proposed a mechanism for the atheroprotective effects of PPAR γ and its ligands [59], demonstrating that troglitazone significantly reduced the number of macrophages within atherosclerotic lesions in both nondiabetic and diabetic mice. Rosiglitazone was also shown to limit lesion formation in LDL-C receptor deficient mice [60], and similar results were reported in apoE knockout mice [61]. Therefore, PPAR γ agonists seem to inhibit early lesion formation possibly through interference of monocyte transendothelial migration with or without insulin resistance. Because PPAR γ was able to exhibit similar effects in diabetics and nondiabetics, its ligands seem to have separate antiatherogenic activities in addition to their insulin sensitizing effects. To further elucidate these protective effects and the ability to use PPAR γ ligands as a therapeutic tool, not only for the treatment of type 2 diabetes but also as a prophylactic for the progression of atherosclerosis, one needs to assess the ability of PPAR γ ligands to affect clinical endpoints of atherosclerosis. One of the first clinical studies to evaluate the effects of PPAR γ agonists on atherosclerosis progression was performed using Japanese patients living with type 2 diabetes. These patients were treated with either 30 mg/day of pioglitazone or placebo for six months and carotid intima thickness (IMT) was evaluated at baseline, three months and six months post-treatment. In the placebo group, IMT increased from baseline by an average of about 0.22mm over the six months while

decreasing about 0.084mm in the treatment group. These differences were significant, and demonstrated that PPAR γ agonist treatment could result in early inhibition of normal, atherogenic processes[62].

PPAR γ has also been implicated in the mediation of inflammation and some of the key players in the inflammatory process including CRP. It is well established that inflammation plays a pivotal role in the atherosclerotic process promoting endothelial dysfunction, which triggers a cascade of detrimental processes that lead to the formation of the atheroma [63]. In a study carried out by Haffner et al., it was demonstrated that after 26 weeks of Rosiglitazone treatment in patients with type 2 diabetes, concentrations of mean CRP, MMP-9, and WBC were all significantly decreased [64]. Rosiglitazone had similar effects on CRP levels as well as fibrinogen levels in nondiabetic patients in a study carried out by Sidhu et al., [62]. Several studies have confirmed that CRP, in addition to being a powerful predictive biomarker, is also a mediator of atherosclerosis. CRP has been demonstrated to decrease nitric oxide production, destabilize nitric oxide synthase mRNA, increase endothelial cell apoptosis and increase NF κ B expression [65, 66]. If CRP expression can be decreased through stimulation of PPAR γ , so can the proatherogenic affects mediated by CRP. However, the debate over the involvement of PPAR γ as well as CRP in the initiation and progression of the inflammatory process is still a controversial one. As stated, PPAR γ is expressed in vascular smooth muscle cells, endothelial cells, macrophages and T cells, all integrally involved in the inflammatory cascade. The debate is not over whether or not PPAR γ is expressed in these cells, or even whether or not it is involved in the regulation of the inflammatory response; these are both accepted concepts. The debate stems from the question of whether or not PPAR γ is

an anti- or pro- inflammatory mediator. PPAR γ specific ligands have been shown to inhibit the expression of a host of inflammatory cytokines including TNF- α , interleukin (IL) 1 β and IL6 in monocytes [67], as well as inducible nitric oxide synthase, MMP-9, and scavenger receptor 1 in macrophages [68]. In one study, PPAR γ ligands inhibited angiotensin II (Ang II)-accelerated atherosclerosis in LDL-C Δ - mice, whereas there was no effect on lipid profiles, blood glucoses, or blood pressure. Intriguingly, the attenuation of AngII-accelerated atherosclerosis was correlated with a down regulation of the proinflammatory transcription factor early growth response gene 1 (Egr-1) and several of its target genes [69]. Due to the observation that while blood pressure and glycemic status were unaffected, but progression of atherosclerosis was inhibited, one can tentatively conclude that inhibition of inflammation plays a crucial role in the anti-atherosclerotic affect of PPAR γ ligands. Further work elucidating some of the mechanisms behind the antiinflammatory affects of PPAR γ as well as clinical endpoints of atherosclerosis needs to be carried out in order to characterize PPAR γ 's effect on inflammation and how its regulation of inflammation affects progression of atherosclerosis. Large-scale trials examining the effects of PPAR γ ligands on clinical cardiovascular endpoints are underway, but data is currently being collected from smaller clinical studies in patients with type 2 diabetes. One such study demonstrated that troglitazone and pioglitazone have potent inhibitory effects on the progression of carotid arterial intima-media thickness [70]. Unfortunately, one cannot determine whether the antiatherosclerotic effect observed post administration of the insulin sensitivity treatment was independent of the antidiabetic effects of the drugs. Hypothetically, the reduction in intima media thickness

was caused by a combination of the antiinflammatory effects of the PPAR agonists as well as the confounding effects of increasing systemic insulin sensitivity.

There is also one general effect of PPAR γ activation, not yet discussed, that could also contribute to a decrease in atherosclerotic progression. Most diabetic patients also live with an abnormal lipid profile or chronic dyslipidemia; in addition to endothelial dysfunction, atherogenesis, and thrombosis, insulin resistance causes decreased uptake of free fatty acids (FFA) by adipocytes [71]. Because of increased systemic FFA concentrations, hepatic uptake of FFA also increases, which in turn increases hepatic production of triglyceride-rich lipoproteins, such as very low density lipoprotein (VLDL-C), resulting in a dyslipidemic state. This increase in VLDL-C is also associated with smaller HDL-C particles that are less efficient at the removal of CEs from peripheral tissue including the arterial wall and lipid-laden macrophages. A rise in VLDL-C is also associated with the smaller, denser more atherogenic LDL-C particles that are more susceptible to modification such as oxidation.

The systemic increase in circulating atherogenic lipoproteins and the subsequent rapid uptake leading to foam cell formation is the basis of the atherosclerotic disease state. As stated earlier, at any time, there is a dynamic between the amount of free cholesterol and CEs within the cell. Removal of cholesterol from lipid-laden macrophages within the arterial wall theoretically could lead to the regression of atherosclerosis or stabilization of the plaque. Stabilization of the plaque could prove integral in prophylactically treating patients at high risk of CVD; primarily because of the detrimental results of plaque rupture (stroke, myocardial infarction and all ischemic

diseases). Note the summary below of the effects of PPAR γ on general processes of atherosclerotic development and progression (Table 1).

Stage in atherosclerosis development/progression	Effect of PPAR- γ activation
Lipid oxidation/oxidative stress	<ul style="list-style-type: none"> ↓ gp91^{phox} expression ↓ Oxidative and nitritive species ↓ NOS expression ↑ eNOS activity
Oxidized lipid transport	<ul style="list-style-type: none"> ↑ ABCA1 expression ↑ CD36 expression ↑/↓ CD36 expression depending on insulin resistance status ↓ SRAMII
Chemotraction and inflammation	<ul style="list-style-type: none"> ↓ IFNγ-induced expression of chemokines: IP-10, Mig, and I-TAC ↓ Cytokines: IL-1β, IL-6, TNFα ↓ Inflammatory marker: CRP
Cell adhesion	<ul style="list-style-type: none"> ↓ TNFα-induced expression of VCAM-1 and ICAM-1 ↓ E-selectin and CCR2 expression
Cell migration/proliferation	<ul style="list-style-type: none"> ↓ MMP-9 expression ↑ Cyclin-dependent kinase inhibitor ↓ Retinoblastoma phosphorylation
Thrombosis	<ul style="list-style-type: none"> ↓ PAI-1 expression

ABCA1 = ATP-binding cassette A1; CCR2 = C-C chemokine receptor 2; CRP = C-reactive protein; eNOS = endothelial nitric oxide synthase; ICAM = intercellular adhesion molecule; IFN = interferon; IL = interleukin; iNOS = inducible nitric oxide synthase; IP-10 = IFN-inducible protein of 10 kDa; I-TAC = IFN-inducible T-cell α -chemoattractant; Mig = monokine induced by IFN γ ; MMP-9 = matrix metalloproteinase 9; PAI-1 = plasminogen activator inhibitor type 1; SRAMII = scavenger-receptor-AMII; TNF = tumor necrosis factor; VCAM = vascular cell adhesion molecule; ↑ indicates increase; ↓ indicates decrease.

Table 1: PPAR γ and Atherosclerosis

Derived from Halabi et al.[43]

The involvement of NF-kB, PPARs and other transcription factors in human inflammation and disease certainly establishes them as targets for therapeutics. Indeed, many common synthetic (e.g., aspirin), and traditional (e.g., green tea, curcumin) remedies target, at least in part, the NF-kB signaling pathway. It is likely that our knowledge of the molecular details of these pathways will enable us to develop more specific and potent NF-kB inhibitors. The power and control of these transcription factors in the regulation of the pathology of many disease states is quite evident, which turns us to some of the genes downstream that are activated through these cascades.

ATP Binding Cassette Transporter A1 (ABCA1)

Having the ability to enhance cholesterol efflux from foam cells and facilitate its return to the liver for processing could potentially be a target for drug therapy in the treatment of atherosclerosis. About 7 years ago, Bodzioch et al. [72] were able to identify the molecular defect in Tangiers disease, namely ABCA1. Patients living with Tangier disease (TD) present with low levels of HDL-C and increased sterol accumulation in macrophages putting them at an increased risk for developing CVD. ABCA1 is a membrane transporter abundant in macrophages and expressed ubiquitously that mediates the cholesterol and phospholipid (PL) efflux to lipid poor apoA1, the precursor of HDL-C, and hence plays a major role in reverse cholesterol transport and general cholesterol homeostasis (see figure 3) [73].

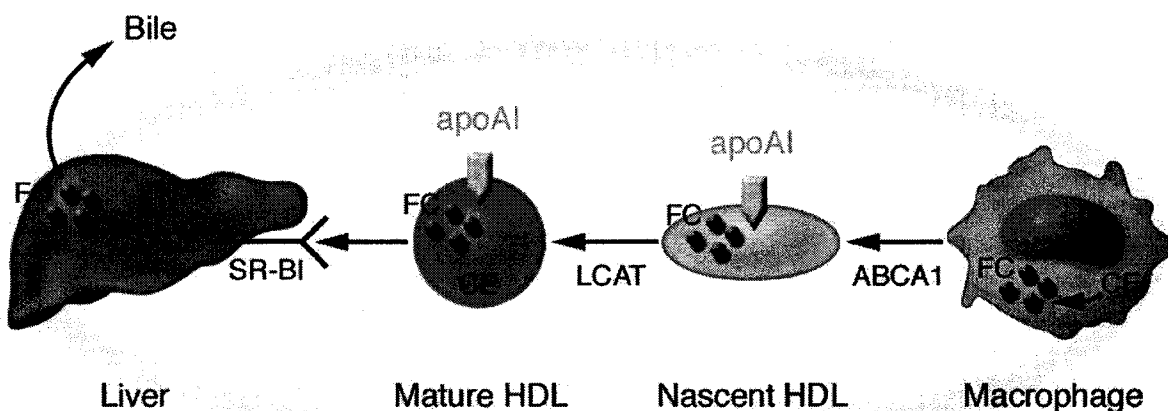


Figure 3: ABCA1 in Reverse Cholesterol Transport [74]

CE=Cholesteryl Ester, HDL=High Density Lipoprotein, LDL-C=Low Density Lipoprotein, FC=Free Cholesterol, SRBI=Scavenger Receptor B1, ABCA1=ATP Binding Cassette A1, LCAT=Lecithin cholesterol acyltransferase

The structure of ABCA1 is characterized by the presence of two transmembrane domains with six helices each, and a nucleotide binding domain containing two conserved peptide motifs that are characteristic for the superfamily of ABC transporters. The membrane transporter also contains two large extracellular loops joined by a disulfide linkage which are thought to be important in the binding of apoA1. Cholesterol efflux from the cell occurs through multiple pathways, ABCA1 being one of them. The efflux of FC promoted by ABCA1 is considered to be unidirectional and occurs through active transport to apoA1, the most abundant apolipoprotein in HDL-C. Recent work suggests that ABCA1 mediates simultaneous transport of FC and PL to apolipoproteins based on the availability of different lipoproteins in the vicinity of the transporter itself; the local discrimination of ABCA1 may result in modification of the ratio of cholesterol /phospholipid undergoing efflux. Recent work has also shown that affecting the PL/apoA1 ratio could play a major role in directing FC efflux through either the ABCA1 or the scavenger receptor B1 (SR-B1) pathway[75]. The apoA1 concentration in the extracellular fluid is dependent on synthesis, catabolism, and dissociation. ApoA1's availability is also dependent on its reassociation with the lipoproteins in the plasma compartment represented by the HDL-C fraction, which in turn could potentially influence lipid efflux from the atheroma.

As stated earlier, the atherosclerotic plaque is a dynamic, multi-factorial environment in which multiple mechanisms can affect its' progression and stabilization. Some of these mechanisms that may be directly modified by the activation of ABCA1 include: altered extracellular matrix turnover, lipid accumulation and metabolism, and alterations in cell turnover involving apoptosis and inflammation. Apoptosis, or

programmed cell death, plays an important role in regulating and controlling cellular turnover within atherosclerotic plaques. In order for the apoptotic process to be successful as well as immunologically silent, the initial phase must be followed by an efficient phagocytic phase. After initiation, phosphatidylserine (PS), an anionic phospholipid which resides on the inner leaflet, is translocated to the outer leaflet which allows the dying cell to be recognized by the phagocyte. ABCA1 was found to be involved in promoting PS translocation and subsequent engulfment of the apoptotic cells [76]. This work illustrated that phagocytosis is impaired in ABCA1 deficient macrophages and that forced induction of ABCA1 can cause engulfment by cells normally not able to carry out the phagocytic process. The ability of ABCA1 to regulate the apoptotic process, or at least induce the removal of dead cells that have undergone apoptosis, presents a possible mechanism that can be targeted for the prevention of progression and/or regression of the plaque. Advanced atherosclerotic plaques contain high numbers of necrotic or dead cells, and enhancing the body's ability to remove those cells could aid in decreasing the severity of the atheroma.

Since ABCA1 also plays a putative role in inflammation, it may be involved in the pathophysiology of atherosclerosis. A number of inflammatory mediators including interferon-gamma (IFN- γ), TNF α , and IL-1 have been reported to decrease the mRNA and protein expression levels of ABCA1. It has been demonstrated that IFN- γ can cause a 3-fold downregulation of ABCA1 while simultaneously increasing ACAT activity, thus promoting atherosclerosis. Also, IL-1 β , an activator of matrix metalloproteinases (MMPs) and other interleukins have also been reported to inhibit ABCA1 function thus inducing cellular lipid accumulation [77]. Although the role of ABCA1 in the transport

and expression of the pro-inflammatory cytokines still needs further elucidation, it could be speculated that a detrimental cycle might exist in which the initial activation of macrophages and stimulation of cytokine release could cause ABCA1 deficiency. This “relative deficiency” of ABCA1 could potentially lead to decreased clearance of apoptotic and necrotic cells which in turn could further aggravate inflammatory mediators leading to plaque instability. Based on its antiinflammatory and apoptotic properties, therapeutic regulation of ABCA1 expression could be a promising target in the treatment of atherosclerosis [24].

As discussed earlier, removal of peripheral cholesterol from extra-hepatic tissue is important in controlling the amount of lipid within the central core of the plaque. The process of reverse cholesterol transport is carried out by ABCA1 dependent and independent mechanisms. ApoA1 that is regenerated from HDL-C, or secreted by the liver, is lipidated by ABCA1 in peripheral tissue to form pre- β HDL-C which then can collect cholesterol from extra-hepatic cells. It is also thought that cholesterol processed from LDL-C uptake in the liver is transferred to HDL-C by hepatic ABCA1 to be converted into bile for secretion, a process that is beneficial to atherosclerotic progression. In the Framingham Heart Study [78], a 2-3 fold increase in cardiovascular disease was observed in TD patients and obligate ABCA1 heterozygotes as compared to age and sex matched controls. Another recent study found that patients with ABCA1 mutations had decreased amounts of cholesterol efflux, lower HDL-C concentrations and greater carotid-intima-media thickness as compared to matched controls [79].

Cumulatively, these studies imply a generalized anti-atherogenic effect of ABCA1 via its

contribution to HDL-C formation while macrophage-bound ABCA1 provides a peripheral anti-atherogenic effect on the vasculature.

PPAR γ and ABCA1: The LXR Connection

As discussed earlier, PPAR γ can work in concert with corepressors and coactivators, binding to DNA response elements in order to initiate a genetic response. PPAR γ can heterodimerize with liver X receptor (LXR), another nuclear receptor belonging to the same superfamily as PPAR γ . The LXR subfamily consists of two members, LXR α and LXR β . LXR α is expressed in an auto-regulated and tissue-specific manner, whereas LXR β is expressed ubiquitously. The LXRs are regulated (ligand bound) by the oxysterols which appear to be produced in proportion to cellular cholesterol content [80] and have been shown to play an important role in regulating some of the mechanisms that protect cells from increased cholesterol levels. LXRs also positively regulate several intestinal and hepatic genes integral in cholesterol excretion from the body, including Cyp7, the rate limiting enzyme in bile acid synthesis as well as ABCA1. PPAR γ can indirectly enhance cholesterol efflux by inducing the transcription of LXR α and thus ABCA1. Consequently, the concentration of LXR α expressed in macrophages within the plaque is important because of its ability to control ABCA1 dependent cholesterol efflux. LXRs ability to control cholesterol efflux is completely dependent on ligand availability, which can be affected by endogenous homeostasis (i.e., increased fatty acids). LXR α has been shown to upregulate sterol regulatory element binding protein-1 (SREBP-1) which results in increased unsaturated fatty acid synthesis. Unsaturated fatty acids can promote ABCA1 degradation, indicating indirect negative

regulation of ABCA1 by LXR α [80]. This might not seem important, but could prove to be in patients with insulin resistance and type 2 diabetes where increased levels of fatty acids are observed. This degradation of ABCA1 could in turn be counteracted within the atherosclerotic plaque due to the oxysterol-rich environment which would activate LXR α thus upregulating ABCA1. PPAR agonists, like the glitazones used in the treatment of type 2-diabetes, have been shown in vitro to induce cholesterol efflux from macrophages through the activation of ABCA1[81]. This control, interestingly, overrides the inflammatory suppression of ABCA1 by the cytokine IL-1 β [77]. In terms of plaque physiology, this could prove to be very important due to the increase in inflammatory signals observed within the atheroma. Taken together, therapeutic regulation of PPAR γ could have positive independent and ABCA1 associated effects on the initiation and progression of atherosclerotic disease in diabetic and non-diabetic patients.

The purpose of the current study is to examine the effects of hyperglycemia on the atherosclerosis caused by diet induced hyperlipemia. The study will investigate one of the major transcription factors of inflammation and lipid metabolism, PPAR γ , and how its role in inflammation and reverse cholesterol transport may affect the development of atherosclerosis. PPAR γ expression will be compared to ABCA1, an important trans-membrane protein involved in the shuttling of cholesterol from peripheral tissue back to the liver for processing to determine whether this process is affected by the hyperglycemic state.

Objectives:

1. To determine if hyperglycemia is associated with accelerated atherogenesis as indicated by plaque morphology in a hamster model.
2. To determine if the hyperglycemic state is associated with altered levels of expression of PPAR γ in vivo.
3. To determine if expression of hamster ABCA1 is correlated to increased hamster PPAR γ expression in vivo.
4. To determine whether increasing expression of ABCA1 is associated with increasing circulating levels of HDL-C in hyperglycemic Syrian hamsters.

CHAPTER 2

EXPERIMENTAL DESIGN

Forty-six Syrian F1B male hamsters were brought into the animal facilities and allowed to acclimate for one week, after which four groups were established. Half of the hamsters (23) were given a high fat/high cholesterol diet with streptozotocin (STZ) (hyperglycemic/hyperlipemic), while the other half was only fed the high fat diet (hyperlipemic). One half of the animals from each group were treated for 8 weeks, while the other half were treated for 24 weeks. At each time point, hamsters were sacrificed and blood was taken for total cholesterol, blood glucose, HbA1C, triglycerides, HDL-C cholesterol and non-HDL-C cholesterol. Tissue was removed at time of sacrifice and fixed for immunohistochemical analysis or frozen for Western blot and ELISA analysis of ABCA1 and PPAR γ .

Groups:

1. Hyperlipidemic (8 week Control)
2. Hyperglycemic/Hyperlipidemic (8 week Treatment)
3. Hyperlipidemic (24 week Control)
4. Hyperglycemic/Hyperlipidemic (24 week Treatment)

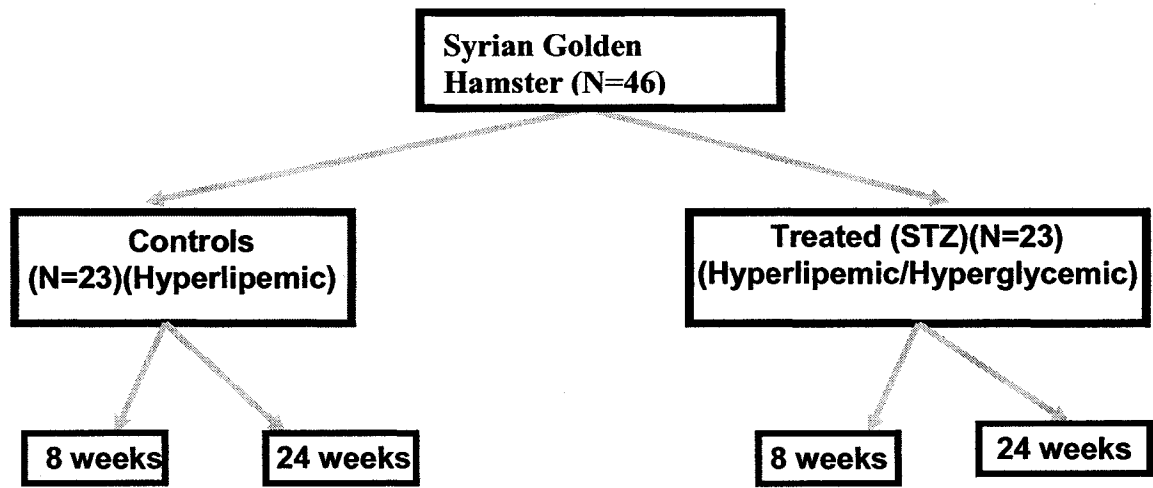


Figure 4: Experimental Design

CHAPTER 3

METHODS AND MATERIALS

Animal Model

The F1B Syrian golden hamster (*Mesocricetus auratus*), as an animal model of atherosclerosis, presents some unique characteristics that are normally unachievable in other rodent models [82]. Hamsters, when fed an atherogenic diet, develop predictable lesions along the inner curvature of the aortic arch in a pathology similar to humans. One hamster study observed fatty streak lesions developing within four weeks of the start of an atherogenic diet and determined that the lesions were morphologically and ultrastructurally similar to human fatty streak lesions [83]. Similar analyses of hamster atherosclerosis have concluded that the lesion development in hamsters progresses through similar stages of progression as compared to humans [84, 85]. Another advantage of the hamster is that the serum cholesterol level increases observed on the atherogenic diet corresponded to an increase in LDL-C and VLDL-C concentrations. This increase is attributable to the fact that, in hamsters, LDL-C is the major plasma cholesterol carrier, which is similar to humans [86]. This increase in LDL-C is not associated with an increase in plasma HDL-C, concomitantly raising their TC/HDL-C ratio. Appropriately, an elevated LDL-C value and a high TC/HDL-C ratio are both significantly associated with the accelerated atherosclerosis seen in humans and the hamster on atherogenic diets [83]. From a practical standpoint, the hamsters are also inexpensive and relatively easy to handle and care for.

By administering STZ, a pancreatic β -cell toxin, the hamster has also been used to study disease associated with a diabetic-like state [87, 88]. Briefly, STZ methylates DNA and generates free radicals ultimately leading to the destruction of the β -cells of the pancreas, responsible for the production of insulin. The STZ Syrian F₁B hamster on a high fat/high cholesterol (atherogenic) diet offers the ability to study the effects of hyperglycemia on the development and pathology of atherosclerosis. STZ has been used to induce a diabetic state in other animal models including the rat and pig [89, 90], but due to their similarities to humans in both lipid profile and metabolism, the hamster may be a more appropriate model to study the connections between diabetes, altered lipid metabolism and accelerated atherosclerosis. The advantage of the hamster was seen in a study by Wang et al. in 2001, in which male Syrian Golden hamsters on a high fat diet were given STZ to induce hyperglycemia. After just two weeks, free fatty acids (FFA), triglycerides and glucose levels all dramatically increased; serum triglyceride was increased by 7.3 fold, FFA by 4.2, and glucose levels by 91% [82]. Due to their similarities in the initiation and progression of atherosclerosis, both physiologically and anatomically, the hyperglycemic hamster provides a unique model in which to study human atherogenic progression in a hyperglycemic state.

Animals

Forty-six Syrian F₁B male hamsters about 8 weeks in age were purchased from BioBreeders Inc. (Fitchburg, MA) and delivered to the laboratory animal research facility

at the University of New Hampshire. The hamsters were housed individually in plastic rodent containers with *ad libitum* access to rodent chow (Purina 5001) and water and maintained on a 12 hour light and dark cycle at $20 \pm 1^\circ$ C. Following a one week acclimation period, hamsters were randomly assigned to one of the four groups 1) 8wk control (C), 2) 8wk treated (T), 3) 24wk control (C) or 4) 24wk treated (T). Following the one week acclimation, all hamsters (N=46), were fed Purina 5001 rodent meal supplemented with 0.25% purified cholesterol (w/w) (Research Diets, Inc., New Brunswick, NJ) and coconut oil 10% (w/w) (Spectrum Organic Products, Inc., Petaluma, CA). The treated hamsters (N=23) were also given an intraperitoneal (IP) injection of STZ (20mg/kg of body weight) (Sigma Chemical, St. Louis, MO) freshly prepared in 0.1M citrate buffer (pH 4.5) with a 22-gauge needle on a 3cc syringe (Becton Dickinson & Co., Rutherford, NJ) one week after arrival at the animal facility. One week after the STZ injection, hamsters were started on their respective diets and continued on those diets for the duration of the study (8 or 24 weeks). All experimental protocols were approved by the Animal Care and Use Committee of the University of New Hampshire (IACUC approval: 040706).

At sacrifice, hamsters were anesthetized using a closed chamber containing isoflurane (Abbot Laboratories, North Chicago, IL). Once the hamsters were immobile, they were removed from the chamber and anesthesia was maintained with a nose cone. Foot reflex and jaw tone were checked to ensure that the animals were deeply anesthetized. The abdomen was rinsed with 70% alcohol and an incision was made in the abdomen through the peritoneum. The ribs were cut to the left of the sternum and hemostats were clamped to the edges of the sternum to expose the heart. Blood was

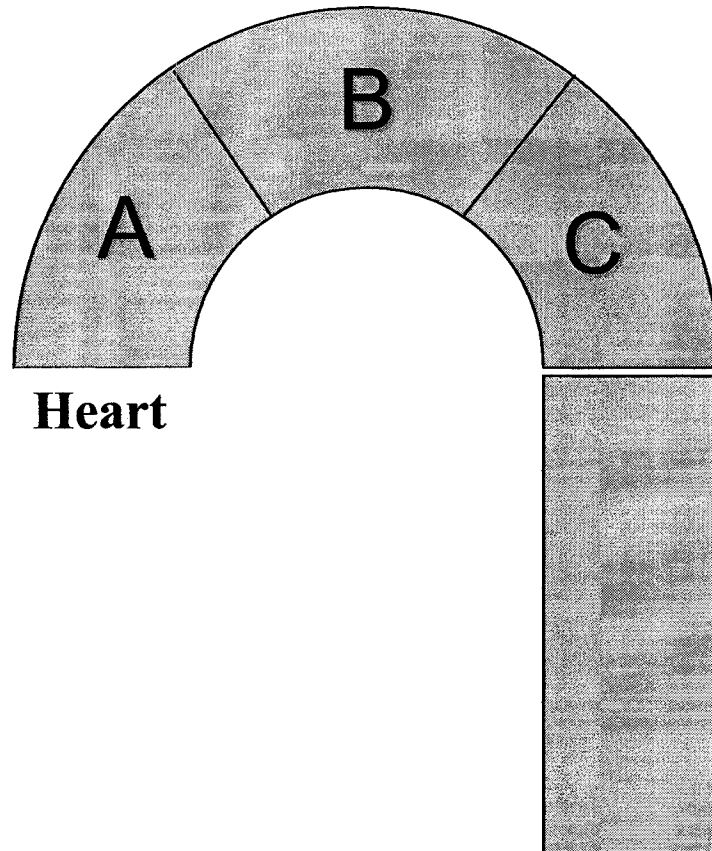
drawn from the left ventricle of the heart with a 22-gauge needle on a 3cc syringe (Becton Dickinson & Co., Rutherford, NJ) and immediately placed into 1.3ml tubes containing 35 I.U. of heparin (Sarstedt, Newton, NC). A small drop of whole blood (~50uL) was used to measure HbA1C and blood glucose levels prior to aliquoting the remaining sample. The samples were then inverted and centrifuged for 12 minutes at 1,500 x g in a table top Eppendorf 5415 microfuge (Brinkman Instruments, Inc., Westbury, NY). Following centrifugation, plasma was aliquoted into microtubes (Sarstedt, Newton, NC) and placed on ice. The samples were stored in a -80° C freezer (Revco Scientific Inc., Asheville, NC) until analysis.

Following the cardiac puncture, a small incision was made in the right atrium for blood outflow, and a 21 gauge 1 inch butterfly needle was inserted into the left ventricle to perfuse the circulatory system. Phosphate buffered saline (PBS) pH 7.4 was continuously infused into the I.V for five minutes at physiologic pressure (110 mm Hg). The fixed hamsters were then perfused for 10 minutes at physiologic pressure with neutral buffered formalin (NBF). All hamsters were then placed on ice until dissection. Both the aortas and the hearts were carefully removed from the formalin fixed hamsters. During dissection, excess adventitia was removed from the aortas to prevent interference during protein analysis. The heart and aorta were kept in-tact, and pinned at in-situ length overnight in 10% NBF. After overnight fixation, the NBF was removed, and the aortic arch was sectioned into three equal pieces (A, B, and C) (figure 5). Each section was placed in a labeled, padded plastic tissue cassette to preserve morphology and rinsed in ddH₂O to wash tissue sections followed by storage in 70% alcohol until processing. Sections were sent to the New Hampshire Veterinary Diagnostic Laboratory (NHVDL)

where they were dehydrated in 100% EtOH and infiltrated with Paraplast Plus™ embedding medium (Oxford Labware, St. Louis, MO) in the Tissue-TeX Automatic Tissue processor (Miles Inc., Diagnostic Division, Tarrytown, NY) overnight. After embedding in paraplast, each tissue section was trimmed and sectioned into 6 micron slices and mounted onto Superfrost/Plus glass slides (Fisher Scientific, Pittsburgh, PA) for immunohistochemical analysis.

Figure 5

Segments of the Hamster Aortic Arch



Segments of the hamster aortic arch: A, B and C are proximal, mid and distal sections respectively. Sections B (mid section) was used for immunohistochemical and histological evaluation and sections A, B and C were used for ELISA and Western Blot analysis.

Immunohistochemistry

Histologic sections from the B or mid portion between the two carotid arteries from each treatment group were incubated with polyclonal antibodies against the antigens for PPAR γ (GENE-TEX, San Antonio, TX) and ABCA1 (ABCAM, Cambridge, UK). The PPAR γ antibody was generated in rabbits against a recombinant protein corresponding to C-terminal amino acids 484-498 of PPAR γ 2. The ABCA1 antibody was also generated in rabbits against a synthetic peptide: AETSDGTL PAP, corresponding to amino acids 1201-1211 of human ABCA1. Reactivity was visualized using the VECTASTAIN® *Elite* ABC Kit (Vector Laboratories, Burlingame, CA) for both ABCA1 and PPAR γ . Briefly, slides were deparaffinized for 20 minutes in two separate toluene baths (10 minutes each), then moved into a series of graded alcohols (10 minutes in 100% ethanol, 10 minutes in 95% ethanol), and re-hydrated in deionized water for 10 minutes followed by a five minute rinse in PBS. Sections were then incubated (for five minutes) in 3% hydrogen peroxide (American Procurement and Logistics Co., Salt Lake City, UT) to eliminate endogenous peroxidase activity, followed by a 5 minute rinse with PBS. Slides were then incubated at 80°C for 10 minutes with Vector Antigen Unmasking Solution (Vector Laboratories, Burlingame, CA) to aid in antigen retrieval. Nonspecific binding was blocked using normal horse serum provided by the VECTASTAIN kit in a 10 minute incubation. Excess serum was blotted using a Kimwipe™ and tissue sections were incubated overnight (18hrs) at 4°C. Serial dilutions were performed in order to determine optimal primary dilutions for both ABCA1 and PPAR γ ; dilution was selected following microscopic evaluation of staining intensity and background. All dilutions were prepared in PBS with 1% BSA and optimal

concentrations chosen were; PPAR γ , 1:500 and ABCA1: 1:50. Optimal primary and secondary dilutions were determined through preliminary work carried out on practice tissue and were chosen based on signal intensity and minimal background appearance. For negative controls, aortic tissue from the hyperglycemic/hyperlipidemic group was used. The treatment tissue was used because we anticipated a stronger antigenic signal as compared to the controls. Negative controls were assessed using PBS, with 1% BSA in lieu of the primary antibody. After overnight incubation, slides were washed for 5 minutes in PBS followed by a 30 minute incubation with provided biotinylated secondary antibody (VECTASTAIN kit). Slides were rinsed for five minutes in PBS, followed by application of an avidin and biotinylated horse radish peroxidase macromolecule complex for 5 minutes followed by another 5 minute rinse in PBS. For visualization of reactivity between the protein of interest and the corresponding primary antibody, the chromagen 3'-amino-9-ethylcarbazole (AEC) (Vector Laboratories, Burlingame, CA), which forms a reddish color upon oxidation by horse radish peroxidase, was applied to the slides for 6 minutes followed by a 5 minute rinse in distilled water. Slides were counter stained with undiluted Gil's hematoxylin for 30 seconds, (Vector Laboratories, Burlingame, CA) rinsed under a gentle tap water stream, and immediately mounted with a glass coverslip and aqueous mounting medium (Zymed, San Francisco, CA).

For morphological examination, B (mid) sections were stained with hematoxylin and eosin (H and E) following deparaffinization and rehydration by the New Hampshire Veterinary Diagnostic Laboratory. Briefly, H and E staining allows for morphologic examination through counterstaining between the nuclei and the cytoskeletal network; hematoxylin stains the nucleic acids (nuclei) blue and the eosin stains the cellulafr

protein (cytoplasm) pink. All slides were examined and photographed using an upright Olympus BH-2 light microscope attached to a digital camera (QImaging Corp, Burnaby, Canada). Images were printed using a 7600 series Hewlett Packard printer (Hewlett Packard Houston, TX) on Canon photo-quality printer paper (Canon, Tokyo, Japan).

Western Blot Protein Analyses

The fixed hearts, aortic arches, and descending aortas and hearts of the hamsters were dissected and removed from the animal at the time of sacrifice. Any excess blood was flushed with PBS and connective tissue was trimmed to avoid background signal. The aortas to be cryo-preserved were cut away from the heart using a sterile razor blade at the point of attachment and placed into separate cryo-vials, flushed with nitrogen, capped and snap frozen in liquid nitrogen. Frozen tissue sections, including aortas were stored at -80° C (Revco Scientific Inc., Asheville, NC) until western blot and transcription factor analyses were performed.

To determine expression of specific proteins within the lesion prone area on the inner curvature of the aortic arch, the thoracic aorta was removed from the heart with a clean razor blade. The descending thoracic aorta was removed from the arch in line with where the proximal portion of aortic arch ended. Western blot analyses for protein expression of PPAR γ were performed on 1 aorta from each treatment group to confirm expression. Aortas were processed and extracted on ice in the cold room at 4° C. To remove excess blood the lumen of the aortas were flushed with PBS using a 1CC syringe. The aortas were minced using a cross-hatch pattern with two clean razor blades on glass slides coated with aminoalkylsilane (Sigma Diagnostics, St.Louis, MO) to prevent tissue

and protein adherence. After mincing, the aortic tissue was moved to a plastic microfuge tube containing 500uL tris buffered saline (TBS) with protease and phosphatase inhibitor mixture (Pierce, Rockford, IL). The aorta was then homogenized with a hand held Tissue Tearor (Dremel, Racine, WI) set at level 30 for 3, 15 second homogenizations with the sample remaining on ice throughout the procedure. Following homogenization, samples were kept on ice for 30 minutes, vortexing every five minutes. After homogenization, samples were pelleted by centrifugation at 500 x g for 3 minutes and supernatant was removed exposing the dry cell pellet in preparation for nuclear extraction. Nuclear extraction was performed using the NE-PER nuclear and cytoplasmic Extraction kit (Pierce, Rockford, IL). Briefly, after concentration of the cell pellet, cytoplasmic extraction reagent (CER) was added to the samples and vigorously mixed by vortexing at the highest setting. After allowing the sample to incubate with the CER, samples were centrifuged at 16,000 x g for five minutes and the supernatant fraction (cytoplasmic fraction) was transferred to a clean, pre-chilled tube. The insoluble pellet, which now contained nuclei, was vigorously mixed with the nuclear extraction reagent by vortexing and allowed to incubate for 40 minutes. The samples were then centrifuged at 16,000 x G for 10 minutes, and the supernatant (nuclear extract) fraction was transferred to a clean, pre-chilled tube and stored at -80 °C until processing. To concentrate tissue samples, aortic tissue was centrifuged, using a 10,000 molecular weight Microcon® centrifugal filter tube device (Millipore Corporation, Bedford, MA), at 13,000 x G for 20 minutes at 4° C. Retentate was then collected via centrifugation at 1,000 x G for 3 minutes at room temperature (RT). The protein concentrations of each sample were determined using the

bicinchoninic acid assay (BCA) (Pierce, Rockford, IL) at 450 nanometers on the ELX800 plate reader (BIO-TEK, Inc., Winooski, VT).

Following protein extraction and quantification, electrophoresis of the proteins was conducted. Equal amounts of total protein were loaded into each lane of every gel for all the aortic samples. The total amount of protein loaded for PPAR and ABCA1 was approximately 7.0ug. Each sample was diluted 1:1 with 2X sample buffer (.5M Tris-HCL, 10% sodium dodecylsulfate, 10% 2-mercaptoethanol, 20% glycerol and 0.02% bromophenol blue) and incubated for 5 minutes in a water bath maintained between 95-100°C. Positive controls, including 3T3 cell extract (Santa Cruz Biotechnology, Santa Cruz, CA), and mouse liver lysate (Santa Cruz Biotechnology, Santa Cruz, Ca) were used for PPAR γ . Samples were allowed to cool to RT and centrifuged to collect condensate prior to loading. 10 uL of each sample was loaded onto 10% tris-HCL gels (Bio-Rad Laboratories, Hercules, Ca). One lane each of Cruz Marker molecular weight markers (5 uL) (Santa Cruz Biotechnology, Santa Cruz, Ca) and Pierce pre-stained marker (5 uL) (Pierce, Rockford, IL) were also loaded onto each gel. A volume of 15 uL of 3T3 cell lysate and mouse liver lysate was loaded onto the gels. Gels were electrophoresed using the Mini-PROTEAN Cell II® system (Bio-Rad Laboratories, Hercules, Ca) for about 50 minutes at 200 volts (Pharmacia Biotech, Uppsala, Sweden). Filter paper, pads and nitrocellulose membranes (Bio-Rad Laboratories, Hercules, Ca) were equilibrated in cold Towban buffer (25mM Tris, 192 mM glycine, 20% methanol, pH 8.3) for 15 minutes. Protein transfer was performed for one hour at 100 volts (Pharmacia Biotech, Uppsala, Sweden). Nonspecific binding was blocked by incubation of blots for one hour in 10% (w/v) nonfat dried milk (Santa Cruz Biotechnology, Santa Cruz, Ca) in TBS (10mM Tris-

HCL, 150mM NaCl, pH 7.4) containing 0.05% (v/v) Tween-20 (TBST) (Bio-Rad Laboratories, Hercules, Ca) on an orbital shaker set between 50-60 rpms at RT. Blots were incubated overnight with primary antibody diluted in 10% (w/v) nonfat dried milk in TBST at 4°C. Optimal primary and secondary dilutions were determined through preliminary work carried out on practice hamster aortic tissue and were chosen based on signal intensity and minimal background appearance. Specifically, goat anti-rabbit PPAR γ (GENE-TEX, San Antonio, TX) was made up at a dilution of 1:1000 in 10% (w/v) nonfat dried milk in TBST. After overnight incubation with primary antibody, blots were washed with a 50ml TBST rinse, followed by 6, 5 minute TBST rinses on an orbital shaker set at 60 rpms. Secondary antibody was diluted with 10% (w/v) non fat dried milk in TBST at the following dilution; 1:10,000 for PPAR γ (donkey anti-goat immunoglobulin G (IgG)- horseradish peroxidase (HRP), Santa Cruz Biotechnology, Santa Cruz, Ca). Blots were incubated with secondary antibody for one hour at RT on an orbital shaker. After incubation, 5, 5 minute 100ml rinses with TBST were performed followed by one more rinse with TBS to minimize background signal during development. West Pico chemiluminescence (Pierce, Rockford, IL) was applied at 10mls per blot and incubated for 5 minutes. Blots were wrapped in Saran Wrap™, exposed to CL-Xposure Film (Pierce, Rockford, IL) and the film was developed using a Konica SRX-101 automated developer.

PPAR γ Transcription Factor Assay (ELISA)

In order to confirm expression and assess relative concentrations of PPAR γ , a 96 well enzyme-linked immunosorbent assay (ELISA) (Cayman Chemical, Ann Arbor, MI)

was used with the nuclear extracts obtained from the aortic tissue. A specific double stranded DNA (dsDNA) sequence containing the peroxisome proliferator response element (PPRE) was immobilized on to the bottom of wells of a 96 well plate. Activated PPARs contained within the nuclear extract, bind specifically to the PPRE. PPAR γ is detected by the addition of a specific primary antibody directed against PPAR γ . A secondary antibody conjugated to HRP is added to provide a sensitive, colorometric reading of absorbance at 450nm. Because the assay was dependent on the binding of PPAR γ to its corresponding response element within the well, the assay specifically measured concentrations of active, bound PPAR γ . The specificity of the assay was confirmed using non-specific binding (NSB) wells to confirm antigen specificity, clarified cell lysate positive control wells, and competitive double stranded DNA (cDNA) wells. Briefly, complete transcription factor binding assay buffer (CTFB) was prepared with ddH₂O, provided assay buffer, and 300mM dithiothreitol (DTT). To the blank wells, and NSB wells, 100ul of CTFB was added, while 90uls was added to the sample and positive control wells, and 80ul was added to the cDNA wells. Following addition of the CTFB, 10 ul of competitor dsDNA was added to the cDNA wells followed by 10 ul of the provided positive control which was also added to the positive control wells. 10ul of each sample was then added to the respective wells, and the plate was allowed to incubate overnight at 4°C. The next day, following a series of washes with provided wash buffer which contained Tween 20 (.5ml/L), primary (1:100) and conjugated secondary (1:100) antibodies were added to all the wells, except for the blanks, and allowed to incubate for one hour at room temperature. Finally, 100ul of developing solution was added to all wells and allowed to incubate with gentle agitation at RT for 45 minutes. Before reading

absorption levels, 100ul of stop solution was added to halt the reaction. The plate was then read at 450 nanometers on the ELX800 plate reader (BIO-TEK, Inc., Winooski, VT), and results were expressed as both OD₄₅₀/ug protein and as a percent of the positive control value.

Serum Assays

Plasma samples were removed from the -80°C freezer and thawed at RT. The following assays were analyzed spectrophotometrically on a Milton Roy spectrophotometer (Milton Roy Company, Rochester, NY) in duplicate and duplicate results averaged prior to statistical analysis. Total cholesterol was measured using the cholesterol oxidase method (Pointe Scientific, Inc., Lincoln Park, MI). Samples that exceeded 700 mg/dl were diluted 1:10 with physiologic saline (.9% NaCl) (The Butler Company, Columbus, OH), vortexed, reassayed and the values multiplied by 10. This was done to bring the measurement into an accurate portion of the standard curve. Triglycerides were determined using the glycerol phosphate oxidase method (Pointe Scientific, Inc., Lincoln Park, MI). Samples that exceeded 1000 mg/dl were diluted 1:10 with physiologic saline (The Butler Company, Columbus, OH), vortexed, reassayed and the values multiplied by 10 to increase accuracy.

Since lipids can impede the transmission of light and yield falsely high numbers, a 'blank' of the lipemic samples was prepared by mixing physiologic saline in lieu of assay buffer with the plasma sample. After the blank was determined, the value was subtracted

from the original values obtained in the assay for both the cholesterol and triglyceride serum plasma assays.

HDL-C Assay

In order to obtain an accurate concentration of serum HDL-C cholesterol, the serum must be combined with a precipitating reagent in order to remove all of the beta lipoproteins (LDL-C and VLDL-C). The HDL-C fraction remains in the supernatant which is drawn off and treated as a sample to be assayed using the enzymatic cholesterol method described above (Pointe Scientific, Inc., Lincoln Park, MI). Briefly, 500 ul of hamster plasma was added to 500 ul of the polyethylene glycol precipitating reagent (Pointe Scientific, Inc., Lincoln Park, MI), and vortexed thoroughly. The sample was then centrifuged for 10 minutes at 2000 x g in a table top Eppendorf 5415 microfuge (Brinkman Instruments, Inc., Westbury, NY). Supernatant was drawn off and placed in respective sample microfuge tubes to be assayed. HDL-C cholesterol was measured using the cholesterol oxidase method (Pointe Scientific, Inc., Lincoln Park, MI), and analyzed spectrophotometrically on a Milton Roy spectrophotometer (spectronic (Milton Roy Company, Rochester, NY) in duplicate and results averaged prior to statistical analysis. Samples were standardized to a 50ug/ml HDL-C standard (Pointe Scientific, Inc., Lincoln Park, MI).

Statistics

GraphPad Prism version V4.0 for Macintosh (Graph Pad Software, Inc., San Diego, California) was used to perform a factorial analysis of variance (ANOVA) followed by Tukey's Multiple Comparison post test to compare groups for all serum

assays and ELISA results. Data are expressed as the mean \pm standard error. Values of $p < 0.05$ were considered statistically significant.

Photo-documentation

Representative slides from the immunohistochemical analysis were examined and photographed microscopically using an Olympus BH-2 microscope at 100X, 200X and 400X with a digital camera (QImaging Corp, Burnaby, Canada) and photo-documented using QCapture version 1.2.0. (QImaging Corp, Burnaby, Canada). Images were printed using a 7600 series Hewlett Packard printer (Hewlett Packard Houston, TX) on Canon photo-quality printer paper (Canon, Tokyo, Japan).

CHAPTER 4

RESULTS

Body Weights

At the beginning of the study, the hamsters weighed an average of 101.6 grams. After 8 and 24 week periods, control groups weighed significantly more ($p < .0001$) than their initial weight (Table 2, Figure 5). Although there was a trend of gradually increasing weights amongst the treatment groups at 8 and 24 weeks, the differences were not significant ($p = .1537$ for 8 week Tx and $p = .4329$ for 24 week Tx).

Selection of Hamsters Based on Response to STZ

Hyperglycemia in response to the i.p. STZ injection varies among animals as has been documented in previous publications [87, 91]. Studies show a direct relationship between HbA1C and average or mean plasma glucose (MPG) levels. For every 1% change in human A1C, there is a change of about 35mg/dl in MPG. Due to wide variations in MPG and more consistent A1C values, HbA1C levels were used to determine the extent of the STZ response. For this study, hyperglycemia was defined as a fasting HbA1C of $\geq 6\%$. The response to the STZ injection, based on elevated HbA1C levels was significant as compared to the control groups who did not receive STZ injections ($p < .0001$). Interestingly, the levels in the 8 week controls were significantly elevated as compared to the 24 week controls ($p < .05$), but no difference was observed in

the 8 week treated group as compared to the 24 week treated hamsters (Table 3, Figure 6).

Plasma Analyses

Lipids

The 8 week control group had the lowest mean plasma total cholesterol values (879.1mg/dL), while the 24 week treatment group had the highest (2474.0mg/dL). Compared to the 8 week control animals, plasma total cholesterol values were significantly higher (2.6 fold) in the 8 week treatment animals ($p < .01$). The 8 week control values were also significantly lower than the 24 week control values ($p < .05$) from animals that consumed the same diet but for a longer period of time. Although there was a trend of higher total cholesterol amongst the 24 week treatments as compared to the 24 week controls, the differences were not significant ($p = .09$). Between the 8 and 24 week treatment groups, there were no differences and no correlative trends (Table 4, Figure 8).

Mean plasma triglyceride values were lowest for the 8 week control animals (707.7mg/dL) and highest for the 8 week treatment animals (3884.0mg/dL) (Table 4, Figure 9). The 8 week treatment group had a 5.5 fold increase for mean plasma triglycerides compared to the 8 week controls which was a significant difference ($p < .01$). Interestingly, there was almost a 2 fold decrease in the mean plasma triglyceride value in the 24 week treatment group as compared to the 8 week treatment group, however, this difference failed to reach statistical significance ($p > .05$). The mean triglyceride level for the 24 week treatment group was two fold higher than the value for the 24 week controls, but also failed to reach statistical significance ($p > .05$).

HDL-C concentrations were lowest in the 24 week treatment hamsters (17.65 mg/dL) and highest in the 8 week control hamsters (57.63 mg/dL) (Table 5, Figure 10). The 24 week treatment hamster values were significantly lower than all other groups ($p < .01$). There was a 2.5 fold difference between the 24 week control and treatment values, which were significantly lower ($p < .001$). Non HDL-C cholesterol values varied from group to group, but exhibited an inverse relationship to the HDL-C cholesterol values. The mean non HDL-C cholesterol value was 3 fold higher in the 8 week treatment hamsters as compared to the 8 week control hamsters ($p < .01$). The 24 week control hamsters had a mean plasma non HDL-C cholesterol level of 1,273 mg/dL as compared to a level of 2,547 mg/dL in the 24 week treatment hamsters which failed to reach statistical significance ($p = .08$). The 8 week controls had significantly lower non HDL-C cholesterol concentrations than the 24 week controls hamsters ($p < .05$). No significant differences were observed when comparing the 8 and 24 week treatment groups. During dissection, it was subjectively observed that the serum from both hyperglycemic groups (8 and 24 weeks) was far more lipemic than the time matched hyperlipemic (control) groups. One commonly used indicator of risk for cardiovascular disease is the ratio of total cholesterol to HDL-C cholesterol levels. The 24 week treatment hamsters exhibited the highest ratio (140.2), while the 8 week controls had the lowest (15.25) (Table 5, Figure 11). The 24 week treatment value was significantly higher than the three other groups ($p < .0001$).

PPAR γ Expression (ELISA)

A PPAR γ transcription factor ELISA was performed and analyzed using nuclear extracts from hamsters from all four groups. Results were expressed as % positive control and as OD₄₅₀/ug protein. No statistically significant differences were observed when comparing treatment and controls within time points or when comparing controls and treatment groups between time points for PPAR γ expression, although presence of active PPAR γ in all four groups was noted (Table 6).

PPAR γ Expression (Western Blot)

PPAR γ expression was not detected through Western Blot analysis. Thirty five micrograms of positive control (3TC cell lysate) was loaded and presence of PPAR γ was confirmed, but we were only able to load approximately 6.5ug of total protein (within nuclear extracts) for each sample in each lane limiting our ability to confirm expression among samples. One possible hypothesis for the lack of reaction seen among sample groups was the minimal aortic tissue size, and even more limited protein concentration following nuclear extraction.

Histology

Mid or B sections (Figure 5) of the aortic arch were examined to evaluate the histology of the aortic wall, and to characterize the stage of lesion development and

relative size. The sections were processed, sectioned and stained with hematoxylin and eosin by the New Hampshire Veterinary Diagnostic Laboratory (Figure 12, N=4).

8 week Control Group: In aortic sections from 8 week control hamsters (n=4) showed few to no fatty streak lesions were observed. Normal morphology was observed with a continuous monolayer of endothelial cells on top of an intact internal elastic lamina (IEL) (Figure 12A).

8 week Treatment Group: Sections of aortic arch from 8 week treatment hamsters (n=4) were examined for lesion development. Some early fatty streak lesions were observed consisting of 1 to 2 layers of subintimal foam cell formation lining the periphery of the luminal space (Figure 12B). The luminal endothelial cell architecture exhibited signs of activation although the monolayer and IEL appeared to be intact.

24 week Control Group: In sections of aortic arch from 24 week control hamsters (n=4), more advanced fatty streak lesions consisting of clusters of 2 to 4 foam cells, attached to the endothelial monolayer, that began to protrude into the luminal space were observed. Foam cells present within the lesions appeared to have increased lipid uptake represented by increased foam cell cytoplasmic volume (Figure 12C).

24 week Treatment Group: Sections of aortic arch from 24 week treatment hamsters (n=4) exhibited more developed and larger fatty streak lesions with clusters of 8 to 15 larger foam cells. Due to foam cell accumulation, lesions protruded well into the luminal space and the nuclei of the foam cells were displaced towards the periphery of the cell. Both the endothelial monolayer as well as the IEL appeared to be intact (Figure 12D).

Immunohistochemistry

Paraffin embedded sections of aortic arch for immunohistochemistry were deparaffinized in toluene, rehydrated and reacted with primary antibodies for PPAR γ and ABCA1. Positive immunoreactivity was monitored by the presence of red chromagen. Representative samples from each group for PPAR γ are presented in figure 14, and figure 15 for ABCA1. Representative negative controls for each antibody are presented in figure 13.

PPAR γ

In the 8 week control group (Figure 14A), the smooth muscle cells exhibited a diffuse immunoreaction for PPAR γ with dispersed chromagen deposition throughout medial and intimal space. PPAR γ immunoreactivity in the 8 week treated (Figure 14B) hamsters was multi-focal and more intense as compared to the 8 week control hamsters. However, the reaction in the treatment hamsters tended to be more localized to the foam cells and prominent endothelial monolayer. The 24 week control hamsters (Figure 14C) had a mild, focal reaction that was localized to the lesion and endothelial monolayer. The 24 week treated aortic sections (Figure 14D) exhibited a multi-focal, intense reaction in the foam cells and a moderate reaction in the SMCs. Thus, although diffuse staining was observed throughout the aortic sections in all groups, the reaction became more intense with increasing development of the lesions.

ABCA1

Immunoreactivity for ABCA1 was present within aortas from all four groups. In the 8 week control hamsters (Figure 15A), there was multifocal to diffuse immunoreactivity for ABCA1 within the endothelial and smooth muscle cells. A slightly more intense reaction was observed in the 8 week STZ treated hamsters both in the endothelial cells and SMCs. The 24 week controls (Figure 15C) had a mild multi-focal reaction throughout the tissue section within all tunicae. Intense, diffuse immunoreactivity was observed in the foam cells of the 24 week treated hamsters (Figure 15D), while moderate multifocal chromagen deposition was observed in the SMCs. Thus, in 8 week treatment and control sections staining is moderately dispersed throughout the endothelial and smooth muscle cell layers. Overall, as fatty streak lesion size increased, there was a concomitant increase in immunoreactivity.

Hamster Weights

Group	Initial Hamster Weights (g)	Final Hamster Weights (g)	% of Gain
8 week Control	93.9	122.9*	30.9
8 week Tx	104.6	112.9	12.9
24 week Control	98.2	130.6*	30.6
24 week Tx	109.5	115.3	15.3

Table 2: Hamster Weights

Values are mean \pm SEM. Values are analyzed for statistical significance with an ANOVA with a Tukey's Multiple Comparison test. Groups with * were significantly heavier at the end of treatment ($p < .0001$).

Serum Assays

Group	Glucose (mg/dL)	HbA1C (%)
8 week Control	289.6 + 34.4 ^a	3.7 + 0.1 ^a
8 week Tx	364.8 + 21.2 ^a	8 + 0.4 ^b
24 week Control	223.4 + 21.2 ^a	3.3 + 0.1 ^a
24 week Tx	328.4 + 31.3 ^b	7.1 + 0.4 ^b

Table 3: Plasma Glucose and Hemoglobin A1C
HbA1C = Hemoglobin A1C

Group	TC (mg/dL)	TRIG (mg/dL)
8 week Control	879.1 + 101.5 ^a	705.7 + 88.8 ^a
8 week Tx	2328 + 442.4 ^b	3884 + 1057 ^b
24 week Control	1425 + 160.3 ^b	1172 + 93.0 ^c
24 week Tx	2474 + 543.4 ^b	2193 + 791.8 ^c

Table 4: Plasma Total Cholesterol and Triglycerides
TC = total cholesterol, TRIG = triglycerides,

HDL-C	Non-HDL-C Cholesterol	TC/HDL-C
57.63 + 18.9 ^a	807.3 + 110.4 ^a	15.25 + .005 ^a
36.36 + 5.6 ^a	2292 + 437.9 ^b	64.03 + .015 ^b
42.94 + 4.0 ^a	1273 + 161.0 ^c	33.19 + .095 ^c
17.65 + 3.3 ^b	2547 + 592.5 ^b	140.17 + .085 ^d

Table 5: HDL/non-HDL Cholesterol and Total Cholesterol/HDL Ratio
HDL-C = high density lipoprotein, TC=Total Cholesterol

Values are mean ± SEM. Values are analyzed for statistical significance with an ANOVA with a Tukey's Multiple Comparison test. Groups with dissimilar superscripts are significantly different (p<.05).

Active PPAR γ Expression (Nuclear Extracts)

N=4	8 week Control	8 week Tx	24 week Controls	24 Week Tx
Averages (%Positive Control)	8.071 \pm 0.07	8.348 \pm 0.05	13.371 \pm 0.20	7.726 \pm 0.06
Averages (OD₄₅₀/ug protein)	0.126 \pm 0.05	0.13 \pm 0.04	0.208 \pm 0.15	0.12 \pm 0.04

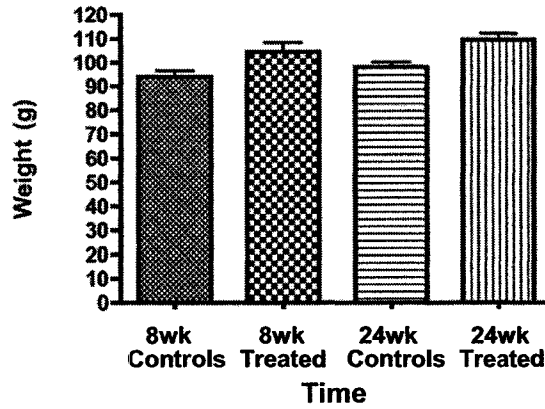
Table 6: Active PPAR γ Expression (ELISA Results)

Values are mean \pm SEM. Values are analyzed for statistical significance with an ANOVA with a Tukey's Multiple Comparison test. Groups with dissimilar superscripts are significantly different (p<.05).

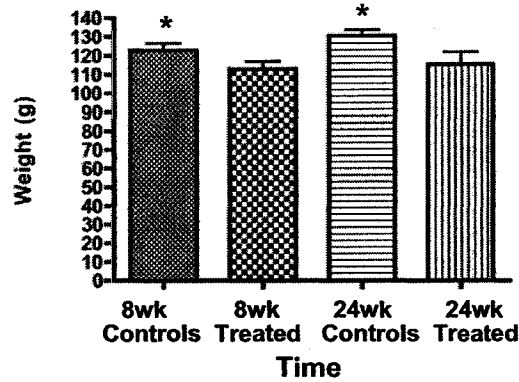
Figure 6

Hamster Weights

Hamster Body Weights at Initiation of Study

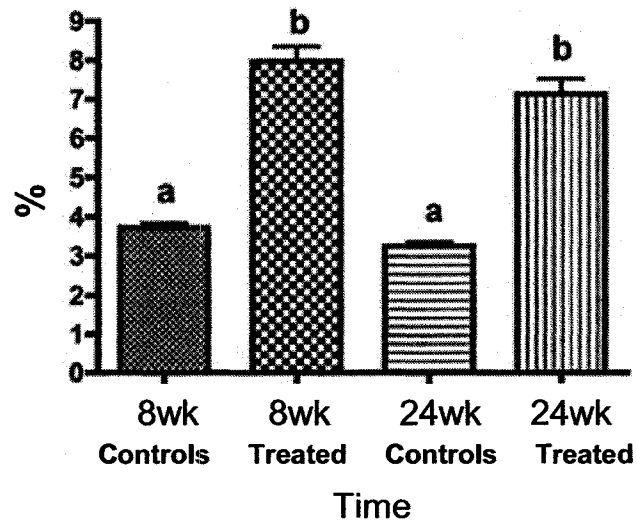


Final Hamster Body Weights at 8 or 24 weeks



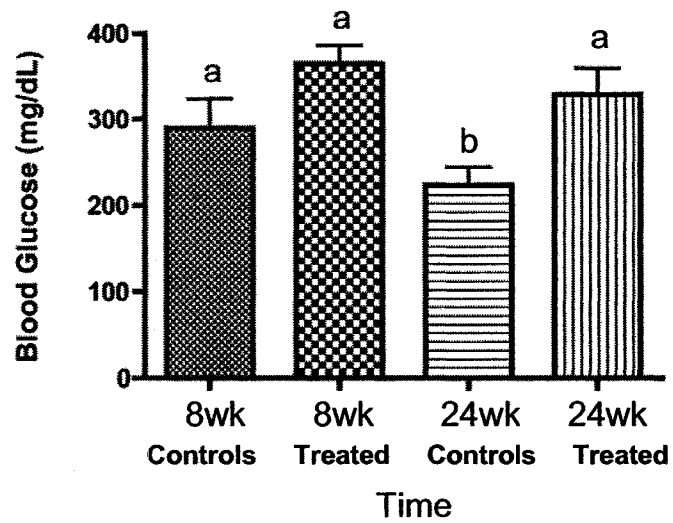
Values are mean \pm SEM. Values are analyzed for statistical significance with an ANOVA with a Tukey's Multiple Comparison test. Groups with * were significantly heavier at the end of treatment ($p < .0001$).

Figure 7
Hemoglobin A1C Values



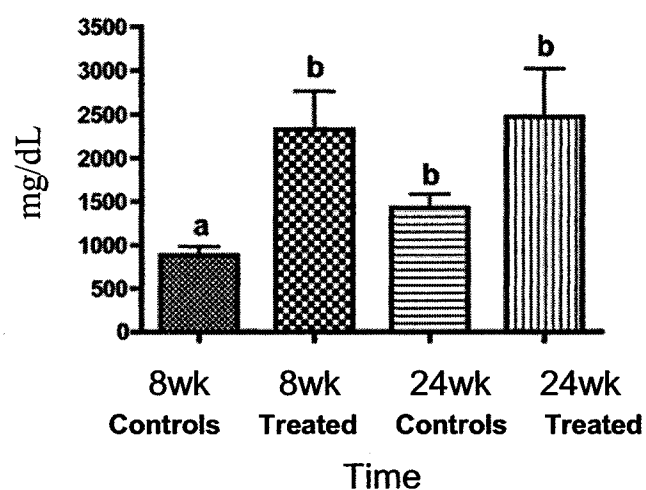
Values are mean \pm SEM. Values are analyzed for statistical significance with an ANOVA with a Tukey's Multiple Comparison test. Groups with dissimilar superscripts are significantly different ($p < .05$)

Figure 8
Blood Glucose Concentrations



Values are mean \pm SEM. Values are analyzed for statistical significance with an ANOVA with a Tukey's Multiple Comparison test. Groups with dissimilar superscripts are significantly different ($p < .05$).

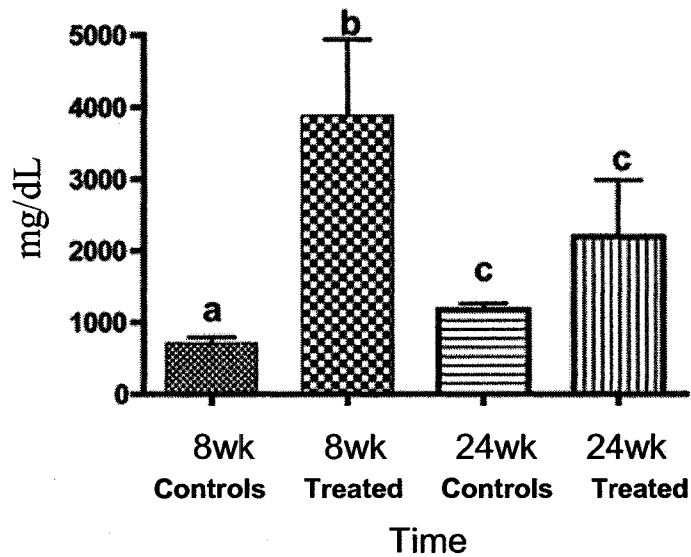
Figure 9
Plasma Total Cholesterol Values



Values are mean \pm SEM. Values are analyzed for statistical significance with an ANOVA with a Tukey's Multiple Comparison test. Groups with dissimilar superscripts are significantly different ($p < .05$).

Figure 10

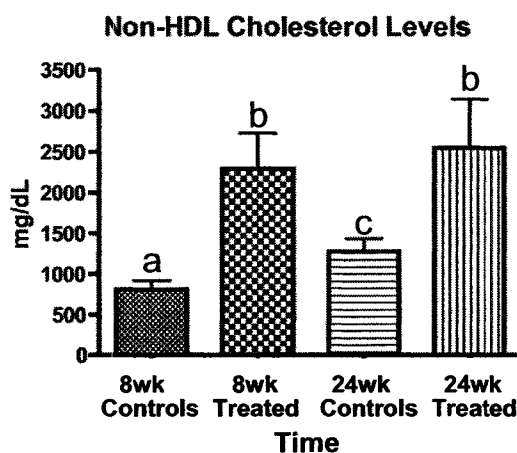
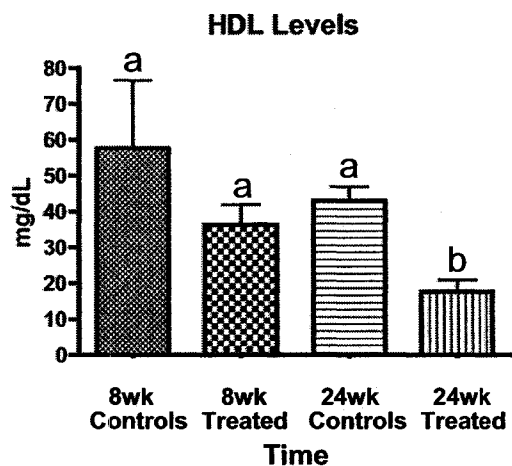
Plasma Triglyceride Levels



Values are mean \pm SEM. Values are analyzed for statistical significance with an ANOVA with a Tukey's Multiple Comparison test. Groups with dissimilar superscripts are significantly different ($p < .05$).

Figure 11

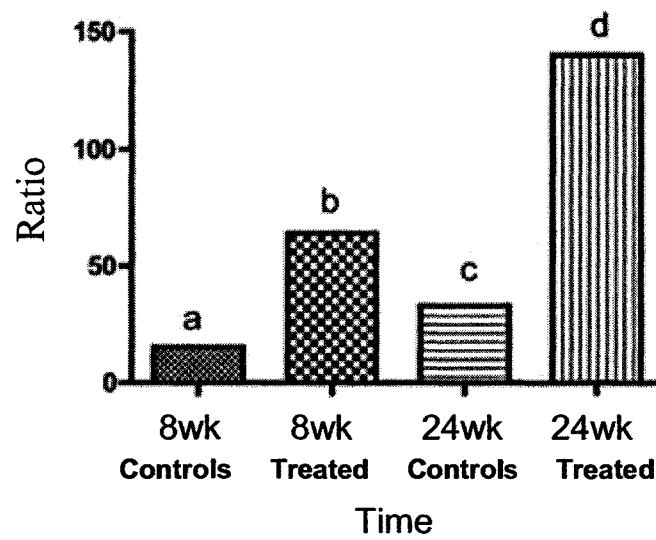
Plasma HDL and Non-HDL Cholesterol Concentrations



Values are mean \pm SEM. Values are analyzed for statistical significance with an ANOVA with a Tukey's Multiple Comparison test. Groups with dissimilar superscripts are significantly different ($p < .05$).

Figure 12

TC/HDL-C Ratio



Values are mean \pm SEM. Values are analyzed for statistical significance with an ANOVA with a Tukey's Multiple Comparison test. Groups with dissimilar superscripts are significantly different ($p < .05$).

Figure 13. Cross-sections of hamster aortic arch (mid section (B)) at 8 and 24 weeks. No lesions were found in the 8 week control sections (A). In the treatment group (8 weeks), early fatty streaks consisting of one or two layers of subendothelial foam cells were observed (B), as the endothelial cells are rested on a prominent, continuous internal elastic lamina. Fully developed fatty streaks were present in the 24 week control hamsters (C). In 24 week Hyperglycemic/Hyperlipidemic aortic sections, (D) advanced fatty streak lesions consisting of several layers of foam cells were present causing a greater protrusion into the luminal space. Again, the IEL remained intact. * indicates localization foam cells. Photographed at 200X.

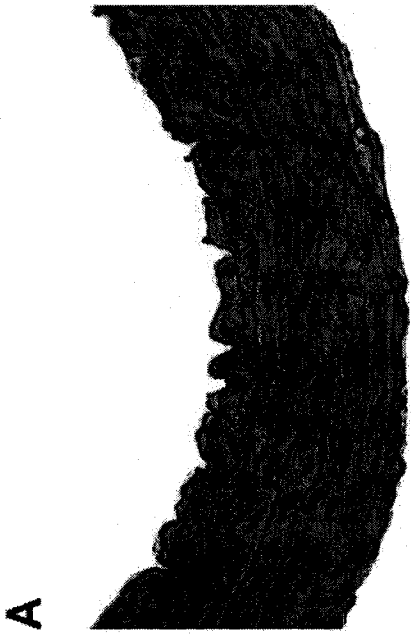
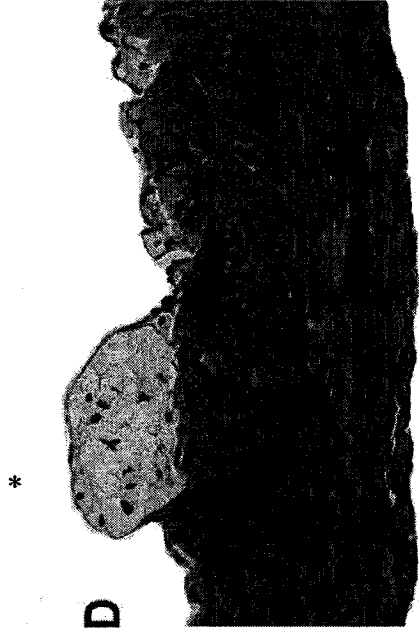
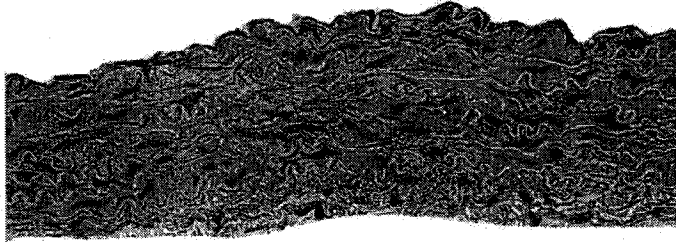


Figure 14. Cross-sections of hamster aortic arch (mid section (B)) at 8 weeks used as negative controls stained for ABCA1 and PPAR γ . In lieu of primary antibody, arterial tissue section was incubated with PBS with 1% bovine serum albumin. (A) is a representative negative control for ABCA1, while (B) is a representative negative control section for PPAR γ . Sections were counterstained with Mayer's hematoxylin. Photographed at 200X.

A



B

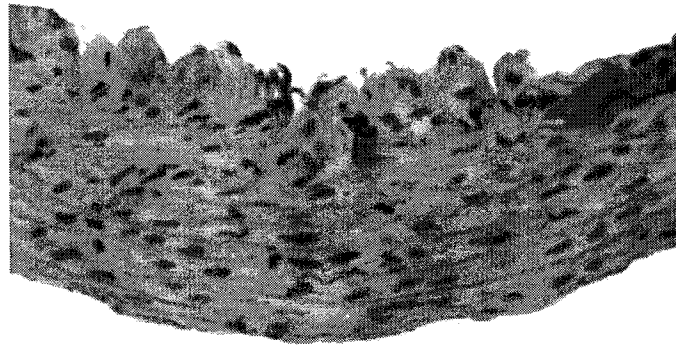


Figure 15. Cross-sections of hamster aortic arch (mid section) immunoreacted with a polyclonal antibody for PPAR γ . 8-week control (A) had multifocal immunoreaction for PPAR γ throughout endothelial cells and smooth muscle cells of the tunica media. A more prominent reaction is observed in the 8-week treatment group (B), with intense immunoreactivity in foam cells and endothelial layer. In the 24-week controls (C), there was moderate, localized immunoreactivity in foam cells and endothelial layer. The 24 week hyperglycemic group (D) had a intense, multi-focal reaction in the foam cells and a moderate reaction in the medial SMCs. All sections were counterstained with Mayer's hematoxylin. Photographed at 200X.

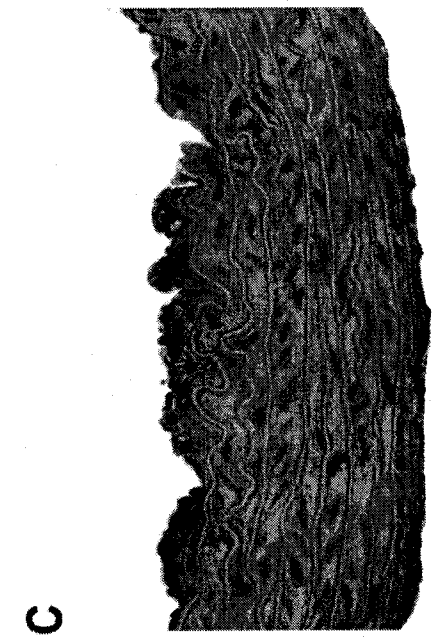
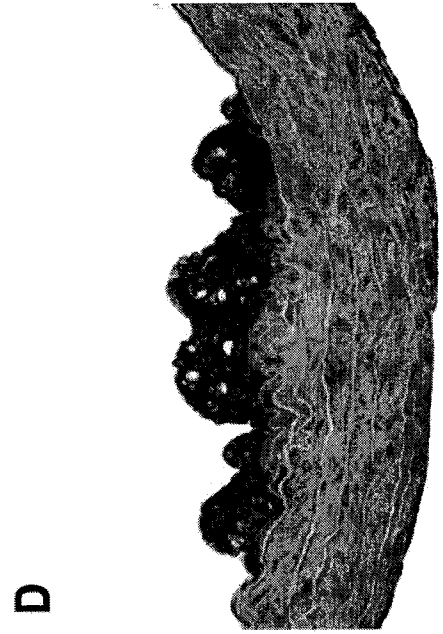
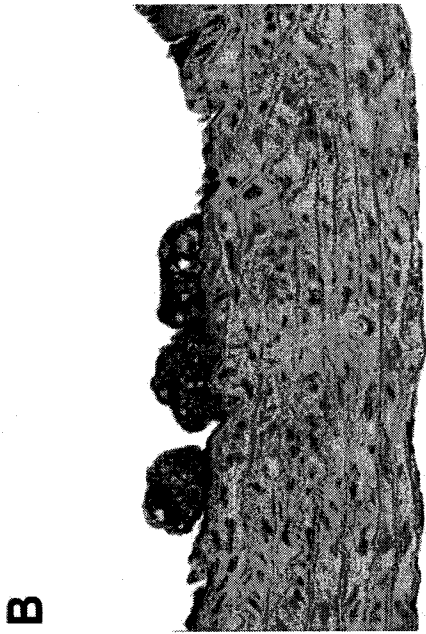
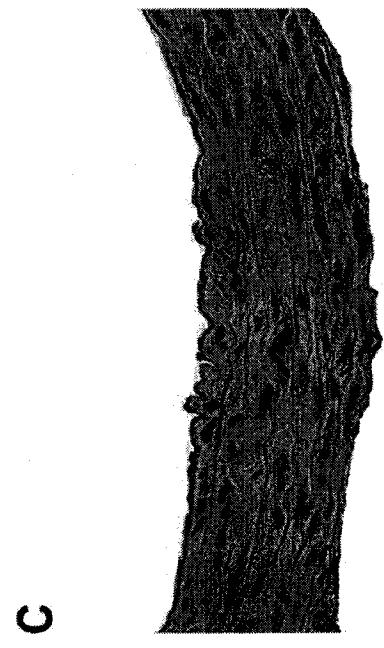
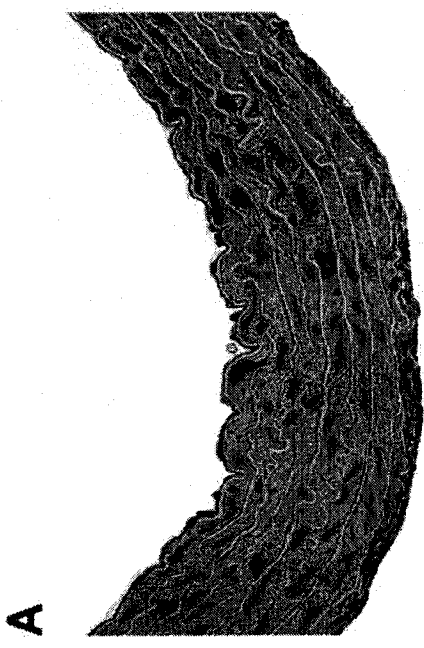
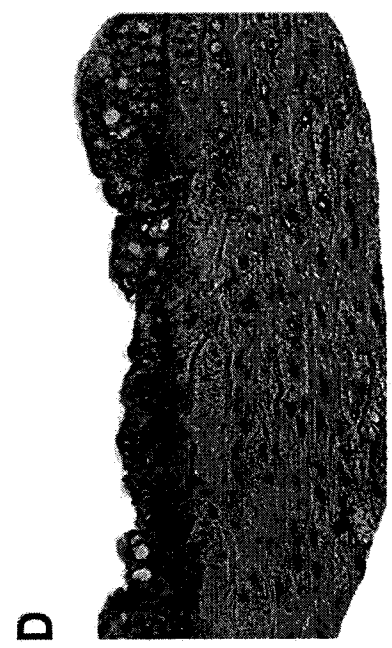
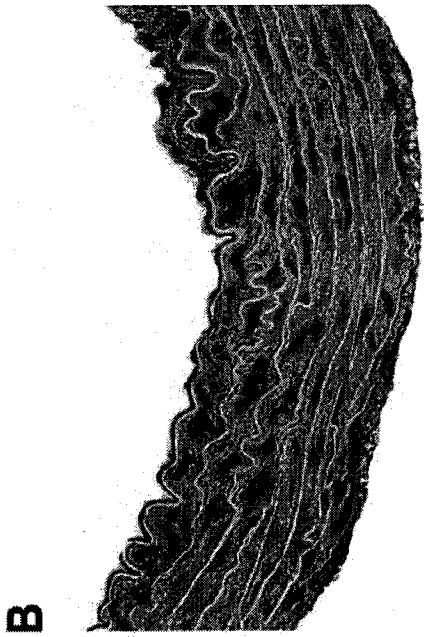


Figure 16. Cross-sections of hamster aortic arch (mid section) immunoreacted with a polyclonal antibody for ABCA1. 8-week controls (A) had multifocal immunoreaction for ABCA1 throughout the endothelium and smooth muscle cells of the tunica media. Intense, multifocal to diffuse immunoreactivity for ABCA-1 was evident in the 8-week treated group (B) in the endothelial cells and throughout the tunica media and adventitia. The 24 week controls (C) had a mild, multi-focal reaction throughout all tunicae. The 24 week treatment group (D) had intense immunoreactivity in the foam cells and moderate, multifocal immunoreactivity in the tunica media. All sections were counterstained with Mayer's hematoxylin. Photographed at 200X.



CHAPTER 5

DISCUSSION

Hyperglycemia, one pathology found in both type I and type II diabetes accelerates the process of atherogenesis in both human patients and animal models [92]. Although the exact mechanism(s) by which hyperglycemia accelerates atherosclerosis is unknown, one possibility may be that the hyperglycemic state effects the activation of inflammatory transcription factors involved in atherogenesis and the progression of atherosclerosis. Hypercholesterolemia, a major risk factor for atherosclerosis, causes focal endothelial activation. When plasma levels of cholesterol-rich LDL-C and VLDL-C become elevated, the lipoproteins infiltrate the artery wall to an extent that surpasses the capacity for removal causing retention within the extracellular matrix [93]. Inflammatory transcription factors, activated upstream, which control genes involved in lipid metabolism may accentuate or attenuate this process of cholesterol deposition and atherosclerotic initiation. This is an initiating step in atherogenesis, which if controlled, could lead to diminished progression of atherosclerosis.

In a hamster model of hyperlipemia and combined hyperlipemia and hyperglycemia, we sought to determine how inflammatory transcriptional control involved in the development of atherosclerosis would be affected by hyperglycemia and if it would affect the initiation and progression of atherosclerosis. In the F₁B strain of Syrian golden hamster, feeding a high fat/high cholesterol (atherogenic) diet caused atherosclerotic lesion development in a predictable manner, and with a morphology and pathology similar to humans [83, 94]. In order to create an atherogenic rodent chow,

0.25% cholesterol and 10% fat was added to the chow (w/w). The atherogenic rodent chow contained 23.5% calories from protein, 26.3% calories from fat, 50% calories from carbohydrates and 32.4 mg (.27% w/w) cholesterol. Adding fat and cholesterol to the rodent chow not only promotes the development of atherosclerosis, it also makes the diet more comparable to a typical Western diet. Although the fat and cholesterol content of the hamster diet contains 8% less calories from fat than the typical Western diet, and only 12% of the cholesterol provided by a Western diet, the atherogenic diet correlates more to the “typical American diet” than the normal rodent chow. Fat and cholesterol are frequently added to rodent chow in order to increase insulin resistance and promote the development of atherosclerosis [82, 95, 96]. In one study, after feeding an atherogenic diet for just ten days, total cholesterol, triglycerides and LDL-C levels were all significantly elevated while HDL-C cholesterol decreased in a fashion similar to that seen in humans [82]. It is important to note that the levels of LDL-C cholesterol, the major plasma cholesterol carrier in both the hamster and humans was significantly elevated making them more prone to developing atherosclerosis. Hyperglycemia can also be induced in the Syrian golden hamster through administration of STZ. The hyperglycemic hamster fed a high fat diet provides a unique model to investigate atherosclerosis under “diabetic-like” conditions [87, 90].

With exception of the 8 week control hamsters, all other groups exhibited fatty streak lesion development to varying degrees. In a few hamsters, occasional clusters of foam cells were present, however, in most of the 8 week controls no foam cells or cell pathologies were visible in any of the aortic sections, and it appeared that the hamsters maintained normal endothelial morphology. In the 8 week treatment hamsters, the

endothelial cell architecture was beginning to become more prominent, a sign of activation, although the monolayer and IEL seemed to be intact. At 8 weeks, the hyperglycemic hamsters exhibited early fatty streak lesions, consisting of 1 to 2 layers of subintimal foam cell formation, as has been previously described [83]. The presence of early fatty streak lesions in the 8 week treatment hamsters as compared to the 8 week control hamsters suggested that, even at early stages, hyperglycemia, elevated TG, TC or perhaps all three accelerated atherogenesis in this lipemic hamster model. These morphological differences in lesion development were more pronounced in the 24 week hamsters. The 24 week control hamsters had more extensive mature fatty streak lesions that protruded into the vessel lumen while the 24 week treatment hamster, due to increased lipid uptake, exhibited lesions that protruded into the luminal space with foam cell nuclear displacement. Once again, due to differences in lesion development between the 24 week groups, it appeared that the hyperglycemic conditions and associated altered lipid levels were accelerating lesional progression. To see if the different conditions would affect levels of transcriptional regulators of inflammation, immunohistochemistry (IHC), western blot (WB) and ELISA analyses were performed for the two proteins PPAR γ and ABCA1 which are both associated with lipid metabolism and atherogenic progression [24, 80].

In this study, the 8 week treatment hamsters had significantly higher total cholesterol values than their time matched controls ($p < .01$) placing these hamsters at greater risk for developing atherosclerosis. A similar trend was observed for total cholesterol values amongst the two 24 week groups, although the difference failed to reach statistical significance ($P > .05$). This discordance could be attributed to the extreme

hyperglycemic state (based on elevated BG and HbA1C levels) induced in the 24 week treatment hamsters leading to hypophagia. This decrease in total cholesterol was associated with a concomitant decrease in HDL-C cholesterol exhibiting a possible reason why these diabetic hamsters might have an increased risk for developing CVD. Interestingly, the molar concentration of HDL-C, which contains relatively more protein and phospholipid than LDL-C, is similar to that of LDL-C in the plasma and, because of its smaller particle size, HDL-C is the predominant lipoprotein species in the tissue. Also, it has been shown in older men and women of any age that the inverse relationship of CHD risk with HDL-C is generally stronger than the direct relationship with LDL-C [97]. By assessing fluctuations in HDL-C levels in diabetic patients, physicians may be able to assess the level of risk for developing cardiovascular disease. HDL-C levels in the 24 week hyperglycemic hamsters were significantly lower than all of the other hyperlipemic hamsters providing a possible reason for increased CVD risk amongst diabetic patients. Clinically, physicians often not only rely on levels of total cholesterol and HDL-C cholesterol as indicators of CVD risk, but also the ratio between the two[98]. The TC/HDL-C ratio followed the expected trend for CVD risk, as it was highest in the 24 week treatment hamsters and lowest for the 8 week control hamsters. The elevated TC/HDL ratio in the 24 week treatment hamsters provides further evidence for the added adverse effect of hyperglycemia over time. Plasma triglyceride levels were significantly elevated in the 8 week treatment hamsters as compared to the 8 week controls, an expected result in individuals with diabetes [2]. Fasting plasma triglycerides were also significantly elevated in both 24 week groups as compared to the 8 week controls, exposing them to an increased risk of developing atherosclerosis [38, 99]. This increased

risk associated with elevated triglyceride levels may be attributed to the fact that triglyceride-rich VLDL contribute to the formation of small, dense, atherogenic LDL-C particles. These dense LDL-C particles are not readily cleared by LDL-C receptors causing them to remain in circulation and within peripheral tissue where they are more susceptible to oxidative modification [100]. The hypertriglyceridemic state observed in the hyperglycemic hamsters contributes to the formation of atherogenic LDL-C through increased transfer of cholesterol to LDL-C. Additionally, high triglyceride levels increase VLDL-C secretion from the liver resulting in the exchange of TGs from VLDL-C for cholesterol esters in HDL-C. The triglyceride in the HDL-C particle can be hydrolyzed, which reduces particle size and can affect the binding of the associated HDL-C protein, ApoA-1. Once affinity for ApoA1 is decreased, it may dissociate from HDL-C where is susceptible to metabolism by the kidney [100]. This mechanism contributes to the low levels of HDL-C observed in diabetics with elevated triglycerides [38, 99]. To summarize, elevated triglycerides leads to the formation of atherogenic LDL-C and decreased HDL-C concentrations putting the hyperglycemic hamsters at an increased risk for developing atherosclerosis; this implies that elevated glucose alone can not explain the increased risk.

An intraperitoneal injection of STZ was used to induce hyperglycemia in both the 8 and 24 week treatment groups. STZ is a pancreatic β -cell toxin that causes necrosis or marked degenerative changes in the pancreatic β -cells with nuclear pyknosis and cytoplasmic vacuolization. It has been shown to produce diabetes mellitus in various species including the Syrian hamster [101, 102]. Interestingly, most species have a high acute mortality to the STZ injection, whereas the Syrian hamster exhibits a high survival

rate from STZ induced hyperglycemia [103]. STZ is a methylnitrosurea that is taken in by rodent β -cells possibly by a glucose transporter molecule. In cells, STZ toxin is an alkylating which causes DNA strand breaks activating poly(ADP-ribose) synthase and a subsequent lethal deletion of β -cell nicotinamide adenine dinucleotide (NAD). Previous studies have also attributed the β -cell breakdown to oxidative stress through the formation of reactive oxygen species (ROS); this effect is further amplified by low levels of antioxidant present within β -cell DNA [104]. Regardless of the mechanism involved, the result of STZ injection is elevated blood glucose levels as a result of DNA strand breaks that are lethal to the insulin producing β -cells.

STZ treatment successfully induced a state of hyperglycemia in both 8 and 24 week treated groups. This effect was evident by the significant increase in fasting HbA1C levels in these groups as compared to the control (hyperlipemic) hamsters ($p < .0001$). The 8 and 24 week control groups had mean plasma HbA1C levels of 3.7 and 3.3 % respectively, whereas the hyperglycemic groups at 8 and 24 weeks had mean HbA1C levels of 8.0 and 7.1% respectively (Table 3). HbA1C levels reflect the degree of glycation on hemoglobin and subsequently blood glucose levels over the past 3-4 months. Because of this, we were able to get an accurate assessment of the glycemetic state of the hamsters for the duration of the study, not just at the time they were sacrificed. This is important due to the extent of stress during sacrifice. Anesthesia principally affects glucose metabolism through the modulation of sympathetic tone; however, in vitro evidence exists that insulin secretion is suppressed by inhalational agents. The insulin deficiency as a result of the anesthesia compounds the absolute insulin deficiency present in persons with diabetes, raising the risks of hyperglycemia and ketogenesis [105]. This

effect could result in abnormally high glucose levels in both treatment and non-treatment hamsters during processing. The statistically significant differences in HbA1C levels accurately confirmed that STZ treatment resulted in elevated plasma glucose levels in the treatment groups during the duration of the study. Blood glucose values were far less consistent than the HbA1C values and are only able to depict a “snapshot” of the blood glucose concentration at the time the blood is drawn.

In order to determine whether the hyperglycemia and abnormal lipid profiles correlated to expression of the inflammatory transcription factor PPAR γ , immunohistochemical, ELISA, and western blot analyses were run to determine its general expression as well as expression of its active form. Various studies have indicated the importance of PPAR γ and its function in metabolic homeostasis and inflammatory control, including three studies that independently reported loss-of-function mutations in the ligand binding domain of human PPAR γ [106-108]. These individuals harbor dominant-negative mutant PPAR γ alleles that impair PPAR γ function by greater than 50%. A summary of clinical features amongst these individuals include: early atherosclerosis, dyslipidemia, early hypertension, limb/gluteal lipodystrophy, severe insulin resistance, polycystic ovaries and hepatic steatosis. Most of these subjects had marked and sometimes extreme dyslipidemia that was characterized by high TG and low HDL-C levels, a phenomenon that we observed in our hamsters specifically in the treated groups. This raises the question of whether individuals with hyperglycemia also have modified expression of PPAR γ . As stated earlier, a crucial indication of the importance of PPAR γ was highlighted when it was discovered as the cognate receptor for the insulin sensitizing TZDs [109]. We questioned whether the effects of PPAR γ activation were

important outside of its clinical role as a receptor for TZD ligand activation. Are endogenous levels of PPAR γ affected by glycemic status? Unfortunately, no differences were observed when we ran an ELSIA of representative samples to assess active PPAR γ expression although presence of active PPAR γ was noted in each group. Although the results from the immunohistochemical analysis are technically not quantitative, it was observed that the reaction became more intense with increasing development of the lesions. Because PPAR γ is expressed in adipose tissue, and developing lesions are characterized by influx of lipid, this could possibly explain the increase in immunoreactivity in the developing lesions; the extremely elevated TG levels could also provide substrate for PPAR γ activation. In addition to being present in adipose tissue, PPAR γ is also present in skeletal muscle, as well as within atherosclerotic lesions[45]. Thus, the effects of PPAR γ activation on atherosclerosis are both indirect, improving insulin sensitivity, and direct, affecting gene expression in the vessel wall, or more specifically within atherogenic macrophages. PPAR γ activation regulates both pro- and antiatherogenic genes involved in cholesterol homeostasis. PPAR γ was found to stimulate transcription of the CD36 gene which is a macrophage scavenger receptor that traditionally contributes to foam cell formation and development of atherosclerosis in mice [110]. In concert with the finding that PPAR γ can be activated by the fatty acid metabolites 9- and 13-hydroxyoctadecadenoic acids (9- and 13-HODE) present in oxLDL-C, a PPAR γ cycle has been proposed in which oxidized lipids would induce activity of PPAR γ , leading to the increased expression of CD36, which in turn would increase oxLDL-C uptake. This process would prove detrimental in the progression of atherosclerosis by promoting foam cell formation. PPAR γ has also been shown to induce

expression of LXR α , thereby stimulating expression of ABCA1-dependent cholesterol efflux. Hypothetically, an even more complex cycle might exist in which there is a concomitant increase in CD36 and ABCA1 resulting in clearance of the detrimental lipid within the atheroma to resident macrophages for removal by ABCA1 back to the liver. If these genes were co-stimulated in the manner described, upregulation of PPAR γ would prove beneficial in slowing and possibly reversing lesion progression. In order to test this hypothesis, this study analyzed expression of endogenous lesional ABCA1 expression through immunohistochemical analyses. Although we did not obtain any quantitative results, similar to the immunoreactivity for PPAR γ , ABCA1 reactivity became more intense with increasing development of the fatty streak lesions. Immunoreactivity tended to increase over time (8 to 24 weeks) and with initiation of treatment (STZ). ABCA1 expression and activity at the macrophage and hepatic levels is critical regarding lipid efflux and HDL-C formation which in turn could influence the progression of atherosclerotic plaques. Interestingly, the lowest levels of HDL-C were found in the 24 week treated hamsters, but the most complex lesions were also observed within this group. This begs the question of whether there really is an increased concentration of ABCA1 with increasing complexity of the lesion, and if so, why are HDL-C levels still declining? One possible explanation is the extreme nature with which the lipid profiles were altered. Although activated PPAR γ was detected by ELISA in all groups, there were no statistical differences between them. However, average 8 week treated values were higher than 8 week controls and 24 week controls were higher than both 8 week control and treated aortas. PPAR γ may have the ability to act like a “lipid sensor”, gauging changes in endogenous cholesterol homeostasis. In the hyperglycemic state, lipid profiles

are altered, and concentrations of circulating FFAs are increased. This increase in FFAs, which are endogenous ligands of PPAR γ , could stimulate activation of PPAR γ , causing a downstream upregulation of ABCA1. This mechanism would be activated in times of dyslipidemia as an attempt to positively influence lipid profiles (stimulate HDL formation). But, upregulating ABCA1 could lack a downstream effect due to the extreme alterations observed in the treated animal's lipid levels. Overall, the PPAR-LXR-ABCA1 cascade has a significant role in cholesterol homeostasis and inflammation and there is promising potential for therapeutic manipulation outside of the insulin sensitizing effects of TZDs. Further work needs to be carried out in which other functions of PPAR γ and the cholesterol transporter ABCA1 as well as their pathways are elucidated so that strategies can be developed to prevent atherosclerotic disease and its extensive complications.

Summary:

We found that hyperglycemia and associated altered lipid profiles amplifies the negative effects of a hyperlipidemic diet through increased total cholesterol levels, non HDL-C levels, triglycerides and decreased HDL-C levels. In the present study, hamsters fed the high fat/high cholesterol diet developed early fatty streak lesions consisting of 1 to 2 layers of foam cells. However, the hamsters that were also treated with STZ developed hyperglycemia and larger, more developed lesions. Lesions characteristic of the 24 week treatment hamsters invaded the luminal space of the aorta due to increased lipid accumulation within larger foam cells. One observed possibility for the increase in atherosclerosis in the treated hamsters was the significantly decreased levels of serum HDL-C, the lipoprotein responsible for RCT. Decreased levels of HDL-C might slow the

process of lipid removal from peripheral tissue (e.g. arterial lesions) for processing in the liver. In order to analyze other mediators of the reverse cholesterol transport pathway, this study observed expression of ABCA1. The expression of ABCA1, based on IHC immunoreactivity, seemed to increase with developing complexity of the lesion and with time. Overall, based on IHC immunoreactivity, the 8 week treatment and control sections exhibited staining that was moderately dispersed throughout the endothelial cells and tunica media. As treatment time increased and subsequently lesion size, ABCA1 expression tended to intensify and localize to lipid laded foam cells. This possible increase could represent a feedback mechanism in response to the elevated concentrations of lipid. This study also analyzed expression of the inflammatory, nuclear transcription factor, PPAR γ which has been shown to regulate ABCA1 as wells as other pro- and antiatherogenic genes [45]. Based on our investigation, active PPAR γ expression did not change with fluctuations in glycemic status (without TZD treatment), as we did not find a difference in expression in our treatment hamsters as compared to the euglycemic controls. Overall, it appears that hyperglycemia is amplifying the dyslipidemic affects of a high fat/high cholesterol diet; possibly providing one reason for the associated increased risk of CVD in diabetic individuals. Further work needs to be undertaken to uncover the effects of altered lipid metabolism and RCT in the progression of atherosclerosis.

REFERENCES

1. Thom, T., et al., *Heart disease and stroke statistics--2006 update: a report from the American Heart Association Statistics Committee and Stroke Statistics Subcommittee*. *Circulation*, 2006. **113**(6): p. e85-151.
2. Betteridge, D.J., *Diabetic dyslipidaemia*. *Diabetes Obes Metab*, 2000. **2 Suppl 1**: p. S31-6.
3. Keaney, J.F., Jr., *Atherosclerosis: from lesion formation to plaque activation and endothelial dysfunction*. *Mol Aspects Med*, 2000. **21**(4-5): p. 99-166.
4. Nishigaki, I., et al., *Lipid peroxide levels of serum lipoprotein fractions of diabetic patients*. *Biochem Med*, 1981. **25**(3): p. 373-8.
5. Kirpichnikov, D. and J.R. Sowers, *Diabetes mellitus and diabetes-associated vascular disease*. *Trends Endocrinol Metab*, 2001. **12**(5): p. 225-30.
6. Doi, H., et al., *Remnant lipoproteins induce proatherothrombogenic molecules in endothelial cells through a redox-sensitive mechanism*. *Circulation*, 2000. **102**(6): p. 670-6.
7. Lind, L., *Circulating markers of inflammation and atherosclerosis*. *Atherosclerosis*, 2003. **169**(2): p. 203-14.
8. Beckman, J.A., M.A. Creager, and P. Libby, *Diabetes and atherosclerosis: epidemiology, pathophysiology, and management*. *Jama*, 2002. **287**(19): p. 2570-81.
9. Grundy, S.M., et al., *Diabetes and cardiovascular disease: a statement for healthcare professionals from the American Heart Association*. *Circulation*, 1999. **100**(10): p. 1134-46.

10. McEwen, L.N., et al., *Diabetes reporting as a cause of death: results from the Translating Research Into Action for Diabetes (TRIAD) study*. *Diabetes Care*, 2006. **29**(2): p. 247-53.
11. Fernandez-Real, J.M., et al., *Insulin resistance, inflammation, and serum fatty acid composition*. *Diabetes Care*, 2003. **26**(5): p. 1362-8.
12. Hulthe, J., et al., *The metabolic syndrome, LDL particle size, and atherosclerosis: the Atherosclerosis and Insulin Resistance (AIR) study*. *Arterioscler Thromb Vasc Biol*, 2000. **20**(9): p. 2140-7.
13. Corella, D. and J.M. Ordovas, *The metabolic syndrome: a crossroad for genotype-phenotype associations in atherosclerosis*. *Curr Atheroscler Rep*, 2004. **6**(3): p. 186-96.
14. Alberti, K.G. and P.Z. Zimmet, *Definition, diagnosis and classification of diabetes mellitus and its complications. Part 1: diagnosis and classification of diabetes mellitus provisional report of a WHO consultation*. *Diabet Med*, 1998. **15**(7): p. 539-53.
15. Ford, E.S., W.H. Giles, and W.H. Dietz, *Prevalence of the metabolic syndrome among US adults: findings from the third National Health and Nutrition Examination Survey*. *Jama*, 2002. **287**(3): p. 356-9.
16. Isomaa, B., et al., *Cardiovascular morbidity and mortality associated with the metabolic syndrome*. *Diabetes Care*, 2001. **24**(4): p. 683-9.
17. Gurnell, M., et al., *The metabolic syndrome: peroxisome proliferator-activated receptor gamma and its therapeutic modulation*. *J Clin Endocrinol Metab*, 2003. **88**(6): p. 2412-21.
18. Brewer, H.B., Jr., *High-density lipoproteins: a new potential therapeutic target for the prevention of cardiovascular disease*. *Arterioscler Thromb Vasc Biol*, 2004. **24**(3): p. 387-91.
19. Plump, A.S., C.J. Scott, and J.L. Breslow, *Human apolipoprotein A-I gene expression increases high density lipoprotein and suppresses atherosclerosis in the apolipoprotein E-deficient mouse*. *Proc Natl Acad Sci U S A*, 1994. **91**(20): p. 9607-11.

20. Badimon, J.J., L. Badimon, and V. Fuster, *Regression of atherosclerotic lesions by high density lipoprotein plasma fraction in the cholesterol-fed rabbit*. J Clin Invest, 1990. **85**(4): p. 1234-41.
21. Yancey, P.G., et al., *Importance of different pathways of cellular cholesterol efflux*. Arterioscler Thromb Vasc Biol, 2003. **23**(5): p. 712-9.
22. Williams, D.L., et al., *Scavenger receptor BI and cholesterol trafficking*. Curr Opin Lipidol, 1999. **10**(4): p. 329-39.
23. Chawla, A., et al., *A PPAR gamma-LXR-ABCA1 pathway in macrophages is involved in cholesterol efflux and atherogenesis*. Mol Cell, 2001. **7**(1): p. 161-71.
24. Soumian, S., et al., *ABCA1 and atherosclerosis*. Vasc Med, 2005. **10**(2): p. 109-19.
25. Oram, J.F. and A.M. Vaughan, *ABCA1-mediated transport of cellular cholesterol and phospholipids to HDL apolipoproteins*. Curr Opin Lipidol, 2000. **11**(3): p. 253-60.
26. Castro, G.R. and C.J. Fielding, *Early incorporation of cell-derived cholesterol into pre-beta-migrating high-density lipoprotein*. Biochemistry, 1988. **27**(1): p. 25-9.
27. Marathe, G.K., G.A. Zimmerman, and T.M. McIntyre, *Platelet-activating factor acetylhydrolase, and not paraoxonase-1, is the oxidized phospholipid hydrolase of high density lipoprotein particles*. J Biol Chem, 2003. **278**(6): p. 3937-47.
28. Barter, P.J., P.W. Baker, and K.A. Rye, *Effect of high-density lipoproteins on the expression of adhesion molecules in endothelial cells*. Curr Opin Lipidol, 2002. **13**(3): p. 285-8.
29. Ross, R., *Rous-Whipple Award Lecture. Atherosclerosis: a defense mechanism gone awry*. Am J Pathol, 1993. **143**(4): p. 987-1002.
30. Yamada, Y., et al., *Scavenger receptor family proteins: roles for atherosclerosis, host defence and disorders of the central nervous system*. Cell Mol Life Sci, 1998. **54**(7): p. 628-40.

31. Suzuki, H., et al., *A role for macrophage scavenger receptors in atherosclerosis and susceptibility to infection*. Nature, 1997. **386**(6622): p. 292-6.
32. Paulsson, G., et al., *Oligoclonal T cell expansions in atherosclerotic lesions of apolipoprotein E-deficient mice*. Arterioscler Thromb Vasc Biol, 2000. **20**(1): p. 10-7.
33. Ross, R., *Atherosclerosis--an inflammatory disease*. N Engl J Med, 1999. **340**(2): p. 115-26.
34. Hansson, G.K., *Cell-mediated immunity in atherosclerosis*. Curr Opin Lipidol, 1997. **8**(5): p. 301-11.
35. Libby, P., *What have we learned about the biology of atherosclerosis? The role of inflammation*. Am J Cardiol, 2001. **88**(7B): p. 3J-6J.
36. Lee, R.T. and P. Libby, *The unstable atheroma*. Arterioscler Thromb Vasc Biol, 1997. **17**(10): p. 1859-67.
37. Glass, C.K. and J.L. Witztum, *Atherosclerosis. the road ahead*. Cell, 2001. **104**(4): p. 503-16.
38. Hokanson, J.E. and M.A. Austin, *Plasma triglyceride level is a risk factor for cardiovascular disease independent of high-density lipoprotein cholesterol level: a meta-analysis of population-based prospective studies*. J Cardiovasc Risk, 1996. **3**(2): p. 213-9.
39. Mohamed, A.K., et al., *The role of oxidative stress and NF-kappaB activation in late diabetic complications*. Biofactors, 1999. **10**(2-3): p. 157-67.
40. Mohan, S., et al., *High glucose induced NF-kappaB DNA-binding activity in HAEC is maintained under low shear stress but inhibited under high shear stress: role of nitric oxide*. Atherosclerosis, 2003. **171**(2): p. 225-34.
41. Hajra, L., et al., *The NF-kappa B signal transduction pathway in aortic endothelial cells is primed for activation in regions predisposed to atherosclerotic lesion formation*. Proc Natl Acad Sci U S A, 2000. **97**(16): p. 9052-7.

42. Monaco, C. and E. Paleolog, *Nuclear factor kappaB: a potential therapeutic target in atherosclerosis and thrombosis*. Cardiovasc Res, 2004. **61**(4): p. 671-82.
43. Halabi, C.M. and C.D. Sigmund, *Peroxisome proliferator-activated receptor-gamma and its agonists in hypertension and atherosclerosis: mechanisms and clinical implications*. Am J Cardiovasc Drugs, 2005. **5**(6): p. 389-98.
44. Chawla, A., et al., *Nuclear receptors and lipid physiology: opening the X-files*. Science, 2001. **294**(5548): p. 1866-70.
45. Li, A.C. and W. Palinski, *PEROXISOME PROLIFERATOR-ACTIVATED RECEPTORS: How Their Effects on Macrophages Can Lead to the Development of a New Drug Therapy Against Atherosclerosis*. Annu Rev Pharmacol Toxicol, 2006. **46**: p. 1-39.
46. Marx, N., et al., *Peroxisome proliferator-activated receptors and atherogenesis: regulators of gene expression in vascular cells*. Circ Res, 2004. **94**(9): p. 1168-78.
47. Moller, D.E. and J.P. Berger, *Role of PPARs in the regulation of obesity-related insulin sensitivity and inflammation*. Int J Obes Relat Metab Disord, 2003. **27 Suppl 3**: p. S17-21.
48. Gilde, A.J., et al., *Peroxisome proliferator-activated receptor (PPAR) alpha and PPARbeta/delta, but not PPARgamma, modulate the expression of genes involved in cardiac lipid metabolism*. Circ Res, 2003. **92**(5): p. 518-24.
49. Graham, T.L., et al., *The PPARdelta agonist GW0742X reduces atherosclerosis in LDLR(-/-) mice*. Atherosclerosis, 2005. **181**(1): p. 29-37.
50. Fajas, L., J.C. Fruchart, and J. Auwerx, *PPARGamma3 mRNA: a distinct PPARgamma mRNA subtype transcribed from an independent promoter*. FEBS Lett, 1998. **438**(1-2): p. 55-60.
51. Mukherjee, R., et al., *Identification, characterization, and tissue distribution of human peroxisome proliferator-activated receptor (PPAR) isoforms PPARgamma2 versus PPARgamma1 and activation with retinoid X receptor agonists and antagonists*. J Biol Chem, 1997. **272**(12): p. 8071-6.

52. Li, A.C. and C.K. Glass, *The macrophage foam cell as a target for therapeutic intervention*. Nat Med, 2002. **8**(11): p. 1235-42.
53. Blanquart, C., et al., *Peroxisome proliferator-activated receptors: regulation of transcriptional activities and roles in inflammation*. J Steroid Biochem Mol Biol, 2003. **85**(2-5): p. 267-73.
54. Satoh, H., et al., *Thiazolidinediones suppress endothelin-1 secretion from bovine vascular endothelial cells: a new possible role of PPARgamma on vascular endothelial function*. Biochem Biophys Res Commun, 1999. **254**(3): p. 757-63.
55. Ricote, M., et al., *Expression of the peroxisome proliferator-activated receptor gamma (PPARgamma) in human atherosclerosis and regulation in macrophages by colony stimulating factors and oxidized low density lipoprotein*. Proc Natl Acad Sci U S A, 1998. **95**(13): p. 7614-9.
56. Marx, N., et al., *Macrophages in human atheroma contain PPARgamma: differentiation-dependent peroxisomal proliferator-activated receptor gamma(PPARgamma) expression and reduction of MMP-9 activity through PPARgamma activation in mononuclear phagocytes in vitro*. Am J Pathol, 1998. **153**(1): p. 17-23.
57. Marx, N., et al., *PPARalpha Activators Inhibit Tissue Factor Expression and Activity in Human Monocytes*. Circulation, 2001. **103**(2): p. 213-219.
58. Yoshimoto, T., et al., *Vasculo-protective effects of insulin sensitizing agent pioglitazone in neointimal thickening and hypertensive vascular hypertrophy*. Atherosclerosis, 1999. **145**(2): p. 333-40.
59. Collins, A.R., et al., *Troglitazone inhibits formation of early atherosclerotic lesions in diabetic and nondiabetic low density lipoprotein receptor-deficient mice*. Arterioscler Thromb Vasc Biol, 2001. **21**(3): p. 365-71.
60. Li, A.C., et al., *Peroxisome proliferator-activated receptor gamma ligands inhibit development of atherosclerosis in LDL receptor-deficient mice*. J Clin Invest, 2000. **106**(4): p. 523-31.
61. Chen, Z., et al., *Troglitazone inhibits atherosclerosis in apolipoprotein E-knockout mice: pleiotropic effects on CD36 expression and HDL*. Arterioscler Thromb Vasc Biol, 2001. **21**(3): p. 372-7.

62. Sidhu, J.S., et al., *Effect of rosiglitazone on common carotid intima-media thickness progression in coronary artery disease patients without diabetes mellitus*. *Arterioscler Thromb Vasc Biol*, 2004. **24**(5): p. 930-4.
63. Farmer, J.A. and G. Torre-Amione, *Atherosclerosis and inflammation*. *Curr Atheroscler Rep*, 2002. **4**(2): p. 92-8.
64. Haffner, S.M., et al., *Effect of rosiglitazone treatment on nontraditional markers of cardiovascular disease in patients with type 2 diabetes mellitus*. *Circulation*, 2002. **106**(6): p. 679-84.
65. Verma, S., et al., *A self-fulfilling prophecy: C-reactive protein attenuates nitric oxide production and inhibits angiogenesis*. *Circulation*, 2002. **106**(8): p. 913-9.
66. Verma, S., et al., *Endothelin antagonism and interleukin-6 inhibition attenuate the proatherogenic effects of C-reactive protein*. *Circulation*, 2002. **105**(16): p. 1890-6.
67. Jiang, C., A.T. Ting, and B. Seed, *PPAR-gamma agonists inhibit production of monocyte inflammatory cytokines*. *Nature*, 1998. **391**(6662): p. 82-6.
68. Ricote, M., et al., *The peroxisome proliferator-activated receptor-gamma is a negative regulator of macrophage activation*. *Nature*, 1998. **391**(6662): p. 79-82.
69. Kintscher, U., et al., *Peroxisome proliferator-activated receptor and retinoid X receptor ligands inhibit monocyte chemotactic protein-1-directed migration of monocytes*. *Eur J Pharmacol*, 2000. **401**(3): p. 259-70.
70. Koshiyama, H., et al., *Rapid communication: inhibitory effect of pioglitazone on carotid arterial wall thickness in type 2 diabetes*. *J Clin Endocrinol Metab*, 2001. **86**(7): p. 3452-6.
71. Ginsberg, H.N., *Insulin resistance and cardiovascular disease*. *J Clin Invest*, 2000. **106**(4): p. 453-8.
72. Bodzioch, M., et al., *The gene encoding ATP-binding cassette transporter 1 is mutated in Tangier disease*. *Nat Genet*, 1999. **22**(4): p. 347-51.

73. Oram, J.F. and R.M. Lawn, *ABCA1. The gatekeeper for eliminating excess tissue cholesterol*. J Lipid Res, 2001. **42**(8): p. 1173-9.
74. Field, J.B., et al., *In vitro and in vivo refractoriness to thyrotropin stimulation of iodine organification and thyroid hormone secretion*. J Clin Invest, 1979. **64**(1): p. 265-71.
75. Yancey, P.G., et al., *In vivo modulation of HDL phospholipid has opposing effects on SR-BI- and ABCA1-mediated cholesterol efflux*. J Lipid Res, 2004. **45**(2): p. 337-46.
76. Hamon, Y., et al., *ABCI promotes engulfment of apoptotic cells and transbilayer redistribution of phosphatidylserine*. Nat Cell Biol, 2000. **2**(7): p. 399-406.
77. Ruan, X.Z., et al., *PPAR agonists protect mesangial cells from interleukin 1beta-induced intracellular lipid accumulation by activating the ABCA1 cholesterol efflux pathway*. J Am Soc Nephrol, 2003. **14**(3): p. 593-600.
78. Schaefer, E.J., et al., *Coronary heart disease prevalence and other clinical features in familial high-density lipoprotein deficiency (Tangier disease)*. Ann Intern Med, 1980. **93**(2): p. 261-6.
79. van Dam, M.J., et al., *Association between increased arterial-wall thickness and impairment in ABCA1-driven cholesterol efflux: an observational study*. Lancet, 2002. **359**(9300): p. 37-42.
80. Li, A.C. and C.K. Glass, *PPAR- and LXR-dependent pathways controlling lipid metabolism and the development of atherosclerosis*. J Lipid Res, 2004. **45**(12): p. 2161-73.
81. Chinetti, G., et al., *PPAR-alpha and PPAR-gamma activators induce cholesterol removal from human macrophage foam cells through stimulation of the ABCA1 pathway*. Nat Med, 2001. **7**(1): p. 53-8.
82. Wang, P.R., et al., *High fat fed hamster, a unique animal model for treatment of diabetic dyslipidemia with peroxisome proliferator activated receptor alpha selective agonists*. Eur J Pharmacol, 2001. **427**(3): p. 285-93.

83. Pien, C.S., *Characterization of diet induced aortic atherosclerosis in Syrian F1B hamsters*. Journal of Experimental Animal Science, 2002(42): p. 65-83.
84. Yamanouchi, J., et al., *APA hamster model for diabetic atherosclerosis. 2. Analysis of lipids and lipoproteins*. Exp Anim, 2000. **49**(4): p. 267-74.
85. Horiuchi, K., et al., *The effect of probucol on atherosclerosis in streptozotocin-induced diabetic-hyperlipidemic APA hamsters in different stages of atherosclerosis*. Exp Anim, 2002. **51**(5): p. 457-64.
86. Spady, D.K., S.D. Turley, and J.M. Dietschy, *Rates of low density lipoprotein uptake and cholesterol synthesis are regulated independently in the liver*. J Lipid Res, 1985. **26**(4): p. 465-72.
87. Simionescu, M., et al., *Pathobiochemistry of combined diabetes and atherosclerosis studied on a novel animal model. The hyperlipemic-hyperglycemic hamster*. Am J Pathol, 1996. **148**(3): p. 997-1014.
88. Takatori, A., et al., *Protective effects of probucol treatment on pancreatic beta-cell function of SZ-induced diabetic APA hamsters*. Exp Anim, 2003. **52**(4): p. 317-27.
89. Gerrity, R.G., et al., *Diabetes-induced accelerated atherosclerosis in swine*. Diabetes, 2001. **50**(7): p. 1654-65.
90. Ebara, T., et al., *Hyperlipidemia in streptozocin-diabetic hamsters as a model for human insulin-deficient diabetes: comparison to streptozocin-diabetic rats*. Metabolism, 1994. **43**(3): p. 299-305.
91. Yang, H. and J.R. Wright, Jr., *Human beta cells are exceedingly resistant to streptozotocin in vivo*. Endocrinology, 2002. **143**(7): p. 2491-5.
92. Aronson, D. and E.J. Rayfield, *How hyperglycemia promotes atherosclerosis: molecular mechanisms*. Cardiovasc Diabetol, 2002. **1**(1): p. 1.
93. Semple, R.K., V.K. Chatterjee, and S. O'Rahilly, *PPAR gamma and human metabolic disease*. J Clin Invest, 2006. **116**(3): p. 581-9.

94. Nistor, A., et al., *The hyperlipidemic hamster as a model of experimental atherosclerosis*. *Atherosclerosis*, 1987. **68**(1-2): p. 159-73.
95. Dorfman, S.E., et al., *Study of diet-induced changes in lipoprotein metabolism in two strains of Golden-Syrian hamsters*. *J Nutr*, 2003. **133**(12): p. 4183-8.
96. Spady, D.K. and J.M. Dietschy, *Interaction of dietary cholesterol and triglycerides in the regulation of hepatic low density lipoprotein transport in the hamster*. *J Clin Invest*, 1988. **81**(2): p. 300-9.
97. Barter, P., et al., *High density lipoproteins (HDLs) and atherosclerosis; the unanswered questions*. *Atherosclerosis*, 2003. **168**(2): p. 195-211.
98. Siguel, E., *A new relationship between total/high density lipoprotein cholesterol and polyunsaturated fatty acids*. *Lipids*, 1996. **31 Suppl**: p. S51-6.
99. Gotto, A.M., Jr., *Triglyceride: the forgotten risk factor*. *Circulation*, 1998. **97**(11): p. 1027-8.
100. Ginsberg, H.N., *Diabetic dyslipidemia: basic mechanisms underlying the common hypertriglyceridemia and low HDL cholesterol levels*. *Diabetes*, 1996. **45 Suppl 3**: p. S27-30.
101. Rakieten, N., et al., *Modification of renal tumorigenic effect of streptozotocin by nicotinamide: spontaneous reversibility of streptozotocin diabetes*. *Proc Soc Exp Biol Med*, 1976. **151**(2): p. 356-61.
102. Takatori, A., et al., *Functional and histochemical analysis on pancreatic islets of APA hamsters with SZ-induced hyperglycemia and hyperlipidemia*. *Exp Anim*, 2002. **51**(1): p. 9-17.
103. Ma, P.T., et al., *Mevinolin, an inhibitor of cholesterol synthesis, induces mRNA for low density lipoprotein receptor in livers of hamsters and rabbits*. *Proc Natl Acad Sci U S A*, 1986. **83**(21): p. 8370-4.
104. Gille, L., et al., *Generation of hydroxyl radicals mediated by streptozotocin in pancreatic islets of mice in vitro*. *Pharmacol Toxicol*, 2002. **90**(6): p. 317-26.

105. Halter, J.B. and A.E. Pflug, *Effects of anesthesia and surgical stress on insulin secretion in man*. *Metabolism*, 1980. **29**(11 Suppl 1): p. 1124-7.
106. Barroso, I., et al., *Dominant negative mutations in human PPARgamma associated with severe insulin resistance, diabetes mellitus and hypertension*. *Nature*, 1999. **402**(6764): p. 880-3.
107. Agarwal, A.K. and A. Garg, *A novel heterozygous mutation in peroxisome proliferator-activated receptor-gamma gene in a patient with familial partial lipodystrophy*. *J Clin Endocrinol Metab*, 2002. **87**(1): p. 408-11.
108. Hegele, R.A., et al., *PPARG F388L, a transactivation-deficient mutant, in familial partial lipodystrophy*. *Diabetes*, 2002. **51**(12): p. 3586-90.
109. Lehmann, J.M., et al., *An antidiabetic thiazolidinedione is a high affinity ligand for peroxisome proliferator-activated receptor gamma (PPAR gamma)*. *J Biol Chem*, 1995. **270**(22): p. 12953-6.
110. Febbraio, M., D.P. Hajjar, and R.L. Silverstein, *CD36: a class B scavenger receptor involved in angiogenesis, atherosclerosis, inflammation, and lipid metabolism*. *J Clin Invest*, 2001. **108**(6): p. 785-91.



June 30, 2005

Thomas Foxall
Animal & Nutritional Sciences
Kendall Hall
Durham, NH 03824

IACUC #: 040706
Original Approval Date: 07/21/2004 **Next Review Date:** 07/21/2006
Review Level: D

Project: Receptors for Advanced Glycated End Products (RAGE) in Atherosclerosis

The Institutional Animal Care and Use Committee (IACUC) has reviewed and approved your request for a time extension for this protocol. Approval is granted until the "Next Review Date" indicated above. You will be asked to submit a report with regard to the involvement of animals in this study before that date. If your study is still active, you may apply for extension of IACUC approval through this office.

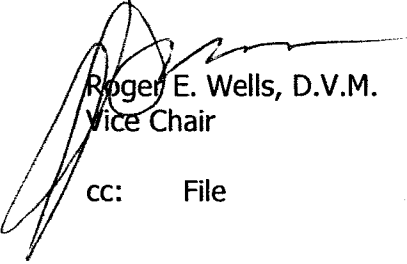
The appropriate use and care of animals in your study is an ongoing process for which you hold primary responsibility. Changes in your protocol must be submitted to the IACUC for review and approval prior to their implementation.

Please Note:

1. All cage, pen, or other animal identification records must include your IACUC # listed above.
2. Use of animals in research and instruction is approved contingent upon participation in the UNH Occupational Health Program for persons handling animals. Participation is mandatory for all principal investigators and their affiliated personnel, employees of the University and students alike. A Medical History Questionnaire accompanies this approval; please copy and distribute to all listed project staff who have not completed this form already. Completed questionnaires should be sent to Dr. Gladi Porsche, UNH Health Services.

If you have any questions, please contact either Van Gouid at 862-4629 or Julie Simpson at 862-2003.

For the IACUC,


Roger E. Wells, D.V.M.
Vice Chair

cc: File